U.S. DEPARTMENT OF COMMERCE
National Technical Information Service

PB-272 423

Synthetic Fuel Production from Solid Wastes

Los Alamos Scientific Lab, N Mex

Prepared for

Municipal Environmental Research Lab, Cincinnati, Ohio

Sep 77

TECHNICAL REPORT DATA (Please read Instructions on the reverse before completing)

PB272423

1. REPORT NO. EPA-600/2-77-147	2.
4. TITLE AND SUBTITLE: SYNTHETIC FUEL PRODUCTION FROM SOLID WASTES	3. RECIPIENT'S ACCESSION NO.
	5. REPORT DATE September 1977 (Issuing Date)
	6. PERFORMING ORGANIZATION CODE
7. AUTHOR(S): Roy C. Feber and Michael J. Antal	8. PERFORMING ORGANIZATION REPORT NO.
9. PERFORMING ORGANIZATION NAME AND ADDRESS: Los Alamos Scientific Laboratory, The University of California, P.O. Box 1663, Los Alamos, New Mexico 87545	10. PROGRAM ELEMENT NO. 505 #1 FY 76/Task 05
	11. CONTRACT/GRANT NO. EPA-IAG-D5-0646
12. SPONSORING AGENCY NAME AND ADDRESS: Municipal Environmental Protection Agency--Cin., OH, Office of Research and Development, U.S. Environmental Research Laboratory, Cincinnati, Ohio 45265	13. TYPE OF REPORT AND PERIOD COVERED: Final Report
	14. SPONSORING AGENCY CODE: EPA/600/14

15. SUPPLEMENTARY NOTES: Project Officer: Albert J. Klee (513-684-7881)

16. ABSTRACT: The work described in this report has two objectives: first, to evaluate potential catalysts for the commercial practice of the gasification of chars produced by the pyrolysis of municipal or industrial wastes; second, to determine the potential for synthetic fuel production from solid wastes produced in this country, and to explore the feasibility of providing the heat required for the gasification reactions by coupling a chemical reactor to a solar collector.

To meet the first objective, a small scale, fixed bed, flow through reactor was assembled, and a number of potential catalysts were tested on chars from a number of sources. The alkali metal carbonates are superior to any of the catalysts for gasification with both steam and carbon dioxide at 650 C. With these catalysts, rates of gasification by steam are increased by factors of two to three, and rates of gasification by carbon dioxide, by factors up to ten. The rates are comparable with those observed elsewhere with other carbonaceous materials.

To meet the second objective, several possible schemes for coupling a solar collector and a gasification reactor are suggested, and economic analyses of the systems are attempted. It is concluded that a feasible, economically attractive systems is possible.

17. KEY WORDS AND DOCUMENT ANALYSIS

a. DESCRIPTORS	b. IDENTIFIERS/OPEN ENDED TERMS	c. COSATI Field/Group
Refuse Pyrolysis Catalysis Methane Hydrogen Carbon monoxide	Pyrolysis char Synthesis gas Monsanto pyrolysis process	7A

18. DISTRIBUTION STATEMENT: RELEASE TO PUBLIC	19. SECURITY CLASS (This Report): UNCLASSIFIED	21. NO. OF PAGES: 47
	20. SECURITY CLASS (This page): UNCLASSIFIED	22. PRICE: $4.00 MF

EPA Form 2220-1 (Rev. 4-77) PREVIOUS EDITION IS OBSOLETE

☆ U.S. GOVERNMENT PRINTING OFFICE: 1977-757-056/6522 Region No. 5-11

PB 272 423

AVAILABLE AT
NATIONAL TECHNICAL
INFORMATION SERVICE
U.S. DEPARTMENT OF COMMERCE
SPRINGFIELD, VA. 22151

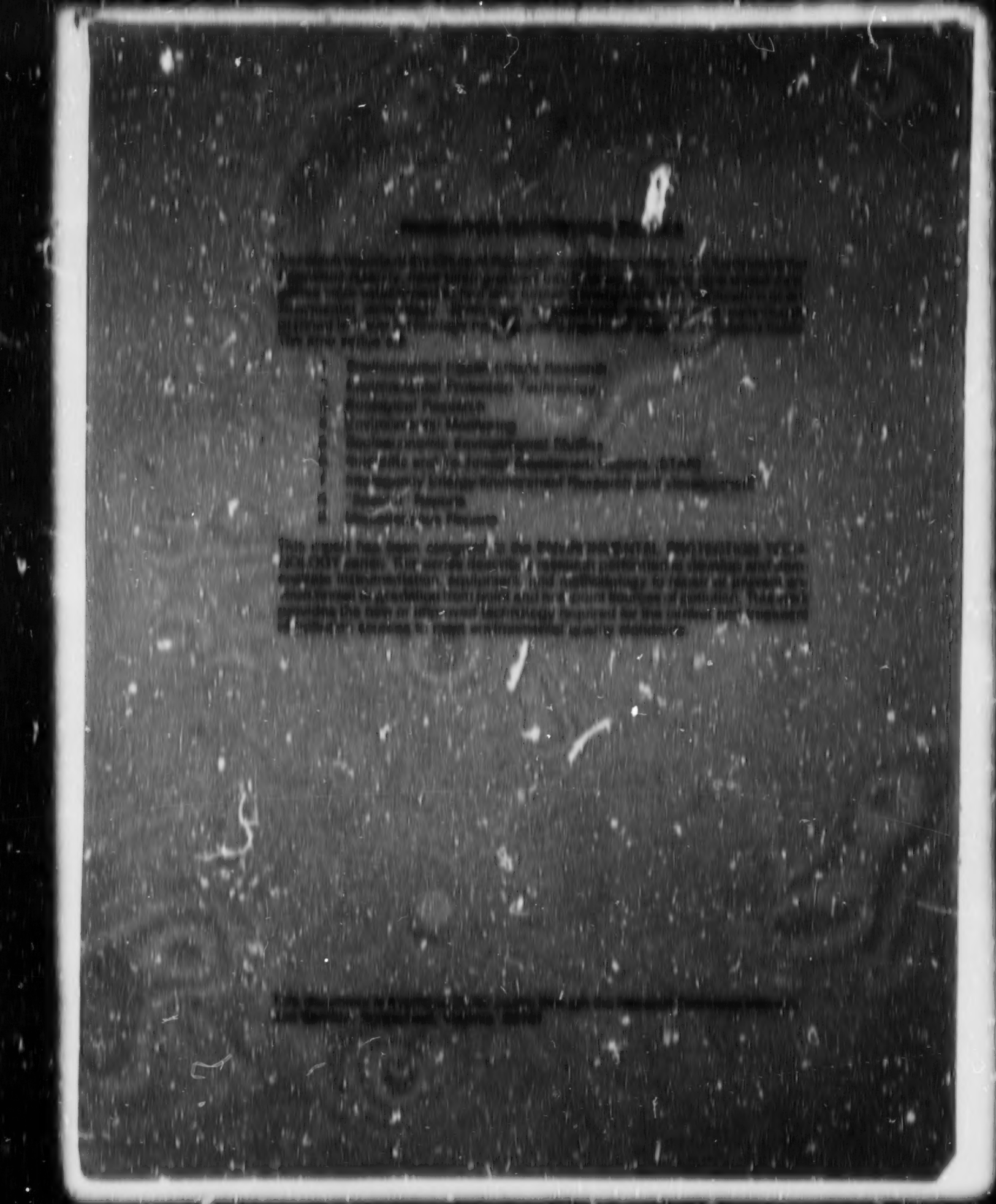

EPA-600/2-77-147
September 1977

SYNTHETIC FUEL PRODUCTION FROM SOLID WASTES

by

Roy C. Feber
Los Alamos Scientific Laboratory
The University of California
Los Alamos, New Mexico 87545

and

Michael J. Antal

Princeton Univ.
Aerospace and Mechanical Sciences Dept.
Princeton, New Jersey.

Interagency Agreement No.
EPA-IAG-05-0646

Project Officer

Albert J. Klee
Solid and Hazardous Waste Research Division
Municipal Environmental Research Laboratory
Cincinnati, Ohio 45268

MUNICIPAL ENVIRONMENTAL RESEARCH LABORATORY
OFFICE OF RESEARCH AND DEVELOPMENT
U.S. ENVIRONMENTAL PROTECTION AGENCY
CINCINNATI, OHIO 45268

DISCLAIMER

This report has been reviewed by the Municipal Environmental Research Laboratory, U.S. Environmental Protection Agency, and approved for publication. Approval does not signify that the contents necessarily reflect the views and policies of the U.S. Environmental Protection Agency, nor does mention of trade names or commercial products constitute endorsement or recommendation for use.

FOREWORD

The Environmental Protection Agency was created because of public and government concern about the dangers of pollution to the health and welfare of the American people. Noxious air, foul water, and spoiled land are tragic testimony to the deterioration of our natural environment. The complexity of that environment and the interplay between its components require a concentrated and integrated attack on the problem.

Research and development is that necessary first step in problem solution and it involves defining the problem, measuring its impact, and searching for solutions. The Municipal Environmental Research Laboratory develops new and improved technology and systems for the prevention, treatment, and management of wastewater and solid and hazardous waste pollutant discharges from municipal and community sources, for the preservation and treatment of public drinking water supplies, and to minimize the adverse economic, social, health, and aesthetic effects of pollution. This publication is one of the products of that research; a most vital communications link between the researcher and the user community.

In particular, this study examines the potential and evaluates the use of char produced from the pyrolysis of solid wastes as a source of synthetic fuel. It reflects our encouragement of greater interest in the use of integrated schemes to meet our future energy requirements in an environmentally acceptable way.

Francis T. Mayo, Director
Municipal Environmental Research
Laboratory

ABSTRACT

The work described in this report has two objectives: first, to evaluate potential catalysts for the commercial practice of the gasification of chars produced by the pyrolysis of municipal or industrial wastes; second, to determine the potential for synthetic fuel production from solid wastes produced in this country, and to explore the feasibility of providing the heat required for the gasification reactions by coupling a chemical reactor to a solar collector.

To meet the first objective, a small scale, fixed bed, flow-through reactor was assembled, and a number of potential catalysts were tested on chars from a number of sources. The alkali metal carbonates are superior to any other catalysts tested for gasification with both steam and carbon dioxide at 650 C. With these catalysts, rates of gasification by steam are increased by factors of two to three, and rates of gasification by carbon dioxide, by factors up to ten. The rates are comparable with those observed elsewhere for other carbonaceous materials.

To meet the second objective, several possible schemes for coupling a solar collector and a gasification reactor are suggested, and economic analyses of the systems are attempted. It is concluded that a feasible, economically attractive system is possible.

This report was submitted in fulfillment of Interagency Agreement EPA-IAG-05-0646 by the Los Alamos Scientific Laboratory under the sponsorship of the Environmental Protection Agency. Work was completed as of December 1975.

CONTENTS

Foreword iii
Abstract iv
Figures vi
Tables vii
Acknowledgment viii

I. Introduction 1
II. Conclusions 4
III. Recommendations 6
IV. Sources and Characterization of Chars 7
V. Experimental Method 23
VI. Experimental Results 29
VII. Systems Study 44

References 69
Appendices

A. Optimization of the reactor's volume 72
B. Radiant heat transfer in gaseous H_2O and $CO_2 + H_2O$ mixture 75

FIGURES

Number		Page
1	Monsanto char carbon of probable biological origin	9
2	Garrett char carbon of probable biological origin	9
3	Monsanto char mineral sperold	10
4	Garrett char miscellaneous fine carbon	10
5	Monsanto char metallic inclusions	11
6	Garrett char bright metallic inclusions	11
7,8	Monsanto char probable pyrolyzed wood	13
9,10	Monsanto char principally inorganic matter	14
11	Monsanto char principally carbonaceous matter	15
12	Garrett char inorganic matter	16
13	Garrett char calcite crystal	16
14,15	Sugar char	17
16	Schematic of gasification reactor tube	25
17	Char reactor equipment	26
18	Reacted uncatalyzed sugar char	36
19,20	Reacted catalyzed sugar char	37
21	Sugar char K_2CO_3 catalyst	38
22	Sugar char Li_2CO_3-K_2CO_3 catalyst	38
23	Sugar char K_2CO_3-DMSO catalyst	40
24	First reactor design	54
25	Second reactor geometry	55
26	Schematic of window assembly	57
27	Schematic of a tubular absorber	61
28	Schematic of a nested annular fluidized-bed reactor	62
29	Light reflection between two mirror surfaces	73

TABLES

Number		Page
1.	Thermodynamics of Char Gasification Reactions	5
2.	Equilibrium Between Char and Steam at 650 C	5
3.	Source and History of PERC Chars	7
4.	Fluorescence Analysis of Inorganic Material in Char	12
5.	Density and Surface Area of Chars	16
6.	Chemical Analyses of Monsanto and Garrett Chars	20
7.	Chemical Analyses of PERC Chars	22
8.	Gasification of Chars to CO by CO_2	31
9.	Gasification of Chars by Steam	33
10.	Removal of Inorganic Constituents from Char by Leaching	41
11.	Recovery of Catalyst Fromars	41
12.	Composition of a Synthetic Solid Waste	42
13.	Analysis of Gas Evolved from Steam-Pyrolyzed Synthetic Solid Waste	43
14.	Average Analysis of Raw Municipal Wastes	46
15.	Hydrogen Production Potential of Wastes Produced in the U. S. A. (1971)	46
16.	Methanol Production Potential of Wastes Produced in the U. S. A. (1971)	47
17.	Mass and Heat Balance Calculations for the Adiabatic System	49
18.	Heliostat Economies of Scale	51
19.	Effect of Temperature on Radiant Heat Loss by Reactor	56
20.	Dimensions of Annular Reactors	67
21.	Economic Analysis of a Municipal Synthetic Fuel Plant	67

ACKNOWLEDGMENTS

The experimental part of this work was done at the Los Alamos Scientific Laboratory, and the systems study was done by Prof. Michael J. Antal.

The authors are indebted to M. C. Tinkle for implementing the experimental part with the assistance of E. Virgil and W. W. Washichek. They also wish to thank Prof. E. F. Thode, New Mexico State University, for his interest and advice.

SECTION I

INTRODUCTION

The pyrolysis of municipal and industrial solid wastes has received considerable attention as an environmentally acceptable alternative to the disposal of such wastes by incineration, open dumping, or as landfill. If, in addition, the useful energy and materials contents of the wastes are regarded as a valuable and renewable national resource, disposal by open dumping or as landfill is clearly undesirable. Also, of course, no volume reduction has been accomplished. Controlled incineration is capable in principle of providing a significant volume reduction and of recovering a significant fraction of the energy content as the heat of combustion. However, additional equipment necessary to make the process thermally efficient and environmentally acceptable is stated to have a relatively high capital cost.

A number of processes have been developed for the pyrolysis, or destructive distillation, of solid wastes, some of which may be regarded as commercial. Much has been written on the subject, and one particularly informative review has been prepared by Huang and Dalton[1]. Most of the processes provide the heat necessary for pyrolysis by partially combusting a portion of the wastes with a sub-stoichiometric amount of oxygen (from air or pure oxygen). Potentially useful liquids or a low Btu gas are produced. In addition a char which may contain 40 to 60% ash remains. It is the utilization of this char to produce a synthetic fuel which is the subject of the present work. If successful, an additional reduction of the ultimate volume of solids to be disposed would also result.

Synthetic fuel may be produced from the carbon contained in char by gasification of the carbon with steam and/or carbon dioxide to produce a gas mixture which also contains hydrogen, carbon monoxide, and methane. The following set of reactions describes the process:

$$H_2O(g) + C(s) \rightleftharpoons H_2(g) + CO(g) \qquad (1)$$

$$CO_2(g) + C(s) \rightleftharpoons 2CO(g) \qquad (2)$$

$$CO(g) + H_2O(g) \rightleftharpoons CO_2(g) + H_2(g) \qquad (3)$$

$$C(s) + 2H_2(g) \rightleftharpoons CH_4(g) \qquad (4)$$

Combining Reaction 1 with the water gas shift reaction, Reaction 3, gives:

$$2H_2O(g) + C(s) \rightleftharpoons CO_2(g) + 2H_2(g) \qquad (5)$$

In a flowing system the proportions of the desirable products hydrogen, carbon monoxide and methane will depend on the temperature and the equilibrium constants and relative rates of the above reactions at that temperature.

In Table 1 are summarized equilibrium constants and the standard enthalpies of Reactions 1-5 from 600 to 1100K. Thermodynamic data for the tables are from the JANAF Thermochemical Tables.[8] The data are based on graphite as the standard state for carbon. Therefore, the numbers will be slightly in error for those reactions involving chars, as the carbon in chars is non-graphitic.

With the exception of Reaction 4, the gasification reactions are endothermic and therefore require an external source of heat. Although the heat might be provided by burning a portion of the char, the premise of this work is that it is preferable to extract a maximum amount of synthetic fuel from the char and that the required heat will be provided by solar process heat. This premise in turn implies that gasification will be done at about 650 C (923 K), a temperature which is regarded as attainable by a reasonable extrapolation of current solar process heat technology. At that temperature the gas compositions shown in Table 2 would be obtained at the indicated pressures if an excess of char were at equilibrium with steam (assuming ideal gas behavior).

These calculations show a very favorable distribution among reaction products at equilibrium at 650 C. In fact, of course, equilibrium with respect to the carbon will not be reached because gasification reactions 1, 2, and 4 are known to be slow, as are reactions in the gas phase involving methane.

One primary objective of this study is therefore to evaluate potential catalysts for the commercial practice of Reactions 1 and 2 when applied to chars resulting from the pyrolysis of municipal or industrial solid wastes. A second objective is to determine the potential for synthetic fuel production from solid wastes produced in this country and to explore the feasibility of providing the heat required for the gasification reactions by coupling a chemical reactor with a solar furnace.

TABLE 1. THERMODYNAMICS OF CHAR GASIFICATION REACTIONS

Equilibrium Constant (pressure in atm.)

T, °K	Reaction* 1	2	3	4	5
600	4.85×10^{-5}	1.71×10^{-8}	28.4	100.	1.38×10^{-2}
700	2.31×10^{-3}	2.43×10^{-4}	9.47	6.93	2.18×10^{-2}
800	4.21×10^{-2}	9.93×10^{-3}	4.24	1.40	0.179
900	0.407	0.176	2.31	0.322	0.941
1000	2.50	1.73	1.44	9.76×10^{-2}	3.60
1100	11.0	11.1	0.993	3.63×10^{-2}	11.0

Reaction Enthalpy, kcal

T, °K	Reaction* 1	2	3	4	5
600	32.168	41.460	-9.292	-19.916	22.876
700	32.307	41.361	-9.050	-20.429	23.251
800	32.391	41.190	-8.799	-20.862	23.592
900	32.442	40.998	-8.540	-21.202	23.896
1000	32.475	40.779	-8.304	-21.482	24.171
1100	32.477	40.543	-8.066	-21.696	24.411

*Reaction

1. $H_2O(g) + C(s) \rightleftharpoons H_2(g) + CO(g)$
2. $CO_2(g) + C(s) \rightleftharpoons 2CO(g)$
3. $CO(g) + H_2O(g) \rightleftharpoons CO_2(g) + H_2(g)$
4. $C(s) + 2H_2(g) \rightleftharpoons CH_4(g)$
5. $2H_2O(g) + C(s) \rightleftharpoons CO_2(g) + 2H_2(g)$

TABLE 2. EQUILIBRIUM BETWEEN CHAR AND STEAM AT 650 C

Pressure, atm	Moles C consumed/ mole added steam	Partial pressure of products, atm: H_2O	H_2	CO	CO_2	CH_4
0.5	0.682	0.051	0.235	0.130	0.062	0.013
1.0	0.619	0.140	0.435	0.210	0.153	0.046
2.0	0.574	0.400	0.760	0.333	0.350	0.141
5.0	0.541	1.341	1.510	0.565	1.026	0.550
10.0	0.530	3.139	2.425	0.828	2.203	1.405

SECTION II

CONCLUSIONS

The alkali metal carbonates are superior to any of the other catalysts tested for gasification by both steam and carbon dioxide. Other catalysts tested included metallic Fe, V_2O_5, $CoMoO_4$, $NiMoO_4$, a zeolite, and fly ash from a coal-fired plant. Because ease of catalyst recovery must be considered for a practicable gasification process, or that catalyst must be inexpensive enough and environmentally acceptable enough to discard, the number of candidates is probably limited, given the present state of the art.

When 10 wt% of the alkali metal carbonates is added to Monsanto or PERC chars, the gasification rates with steam are increased by factors of two to three and those with carbon dioxide by factors to ten. Because uncatalyzed sugar char is less reactive than uncatalyzed Monsanto or PERC chars, its gasification rates are increased by the greatest amount. Acid leaching of ash-containing chars increased slightly reactivity with respect to carbon dioxide, but decreased slightly steam gasification rates.

A comparison of all steam gasification rates suggests that inorganic material in the chars, particularly in Monsanto char for which more data exist, is itself acting as a catalyst for the reaction with steam. Attempts to improve contact of alkali metal carbonate catalysts with chars and thereby enhance gasification rates (by such techniques, for example, as lowering the melting point of the catalyst below the gasification temperature) did, in general, increase the percent conversion of carbon dioxide to carbon monoxide, but were not demonstrably effective in increasing the rate of steam gasification. The general conclusion is drawn that intimate contact between catalyst and char is not critical.

The rates of catalyzed and uncatalyzed reactions tend to decrease with time of gasification. Therefore, to judge if a catalyzed gasification of char can gasify some acceptably large fraction of the available carbon and be an economically competitive source of synthesis gas, some kinetic questions need to be answered.

The major product of steam gasification is a mixture of hydrogen and carbon dioxide at a ratio of about 2:1 with catalyzed and uncatalyzed Monsanto and PERC chars. The amount of carbon monoxide is usually ~2.5%. In the present apparatus the lowest practicable rate of water addition and the rate of steam gasification correspond to a partial

pressure of steam throughout the reaction zone high enough to drive the water gas shift reaction far to the right. Indeed, the amount of carbon monoxide found in the product gas is close to that which would be calculated if the shift reaction were at equilibrium.

The gasification of raw solid wastes produced in this country can make a significant contribution to national hydrogen or methanol requirements.

Several possible schemes for coupling solar collectors to a gasification reactor have been explored for their technical and economic feasibility. Although many engineering features of such systems cannot be specified at present, it is concluded that the development of a commercial solar-steam pyrolysis systems for the production of synthetic fuel from solid wastes deserves further effort.

SECTION III

RECOMMENDATIONS

It has been concluded that alkali metal carbonates have proven their effectiveness as catalysts for the gasification of char by carbon dioxide or steam. However, to determine if the system is a practical one for the production of a synthesis gas and can make an impact on the char disposal problem, further work should be done.

The major thrust of work to be done next should be on engineering kinetic studies. There are three related aspects to the kinetics problem which should be addressed. First, the preponderance of evidence is that char reactivity decreases with reaction time. Therefore it is desirable to define feasible limits to the extent to which carbon may be removed from the chars. Second, in the present apparatus the lowest practicable rate of water addition corresponds to a partial pressure of water high enough to drive the water gas shift reaction far to the right. As a result we produce H_2 and CO_2 at a ratio of near 2:1. A significant concentration of CO would be desirable for a synthesis gas. Assuming that a large scale system would be a flow system, one need to know, for example, the effect of the relative rates of the carbon-steam reaction and the forward and reverse rates of the water gas shift reaction as a function of water partial pressure. These relative rates will determine the $H_2/CO/CO_2$ ratio in the product gas. Third, kinetic data are required for engineering design of a large scale system. A bench scale, stirred-bed, continuous reactor should be capable of providing the necessary data for these purposes.

In addition, it would be appropriate to continue the search for catalysts better than the alkali metal carbonates and for methods of contacting char and catalyst which simplify catalyst recovery procedures.

SECTION IV

SOURCES AND CHARACTERIZATION OF CHARS

SOURCES

Chars from the pyrolysis of solid wastes were obtained from the Monsanto Corporation, the Garrett Corporation, and the Pittsburgh Energy Research Center (PERC). The processes with which these organizations are identified are described in some detail in Volume 2 of Reference 1.

The Monsanto char derived from a pilot plant for the Landgard process, in which pyrolysis takes place at 650 to 980 C. The source wastes are believed to have been municipal wastes. Most of our experimental work was done with this char. The source for the char from the Garrett process was Douglas fir tree bark which had been flash pyrolyzed to about 480 C. Four samples of PERC char were obtained, each of which had a different source and history (Table 3).

TABLE 3. SOURCE AND HISTORY OF PERC CHARS

Code #	Source	Treatment
1221-5	Raw municipal refuse from R.A.M. plant in Altoona, Pa.	Carbonization temperatures between 600°C and 900°C.
1222-6	Same as above, but contains plastic film removed from 1221-5	Carbonized at 750°C.
1223-1	Hell mill industrial refuse.	Carbonized between 600° and 900°C.
1224-3	Gondard mill industrial refuse.	Carbonized at 900°C.

All of the PERC chars were chemically analyzed, but only #1221-5 was used in gasification studies. In contrast with the Monsanto and Garrett

chars, the PERC chars were very heterogeneous and contained large chunks of pyrolyzed material apparently originating from metal, paper, wood, and fabric present in the wastes.

As a reference, ash-free char, a sugar char of high surface area was prepared following directions given in the literature.[3] This procedure required a final temperature of 800 C. Finally, a limited amount of work was done with a char sample produced directly from the steam pyrolysis of a synthetic waste.

CHARACTERIZATION

Microscopic Analysis

A microscopic examination of grab samples of the Monsanto and Garrett chars showed that they are largely composed of amorphous carbon, some of which had a cellular structure indicating carbon of biological origin. There were also some particles that gave metallic reflections and some particles that appeared to be crystalline. Three photomicrographs each of Monsanto and Garrett chars are shown in Figures 1 to 6. Figures 1, 3, and 5 show metallographic sections of the Monsanto char. Figures 2, 4, and 6 are sections of Garrett char. All of the metallographic sections were etched with hydrogen ion bombardment (cathodically vacuum etched with hydrogen) at 3 kV for 15 minutes. Figures 1 and 2 show carbon of probable biological origin in both Monsanto and Garrett chars. In Figure 4 some interesting cubes of mineral matter may be seen in the Garrett char. The mineral matter has a grey intensity in these photomicrographs. In Figures 5 and 6 metallic inclusions are shown in both of the chars. The metallic material shows up as the lightest intensity in the photomicrographs.

Scanning Electron Microscopy

Figure 7 is a photomicrograph of organic constituents in Monsanto char at a magnification of 1000X, and Figure 8 shows the same organic constituents at 3000X. Figure 9 shows a piece of inorganic matter in Monsanto char at 3000X. An electron fluorescence analysis of this piece of material gave as the major components: Mg, Ca, Si, and Al with a trace of Ag. The same piece of material at 10,000X is shown in Figure 10. Figure 11 is of a piece of primarily carbonaceous material with a bright spot of inorganic material in the center. A normalized electron fluorescence analysis of the bright spot is as follows:

Figure 1. Monsanto char. Carbon of probable biological origin. 100X

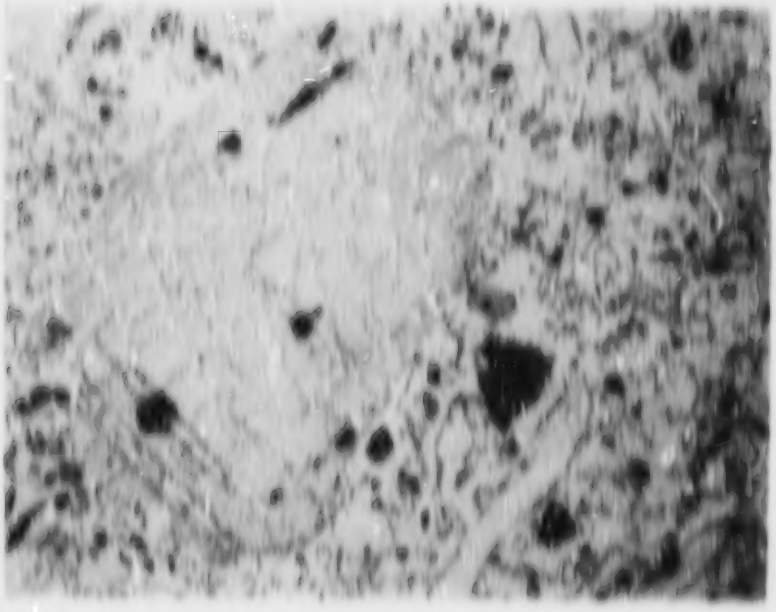

Figure 2. Garrett char. Carbon of probable biological origin 100X

Figure 3. Monsanto char. Mineral spheroid upper left. 100X

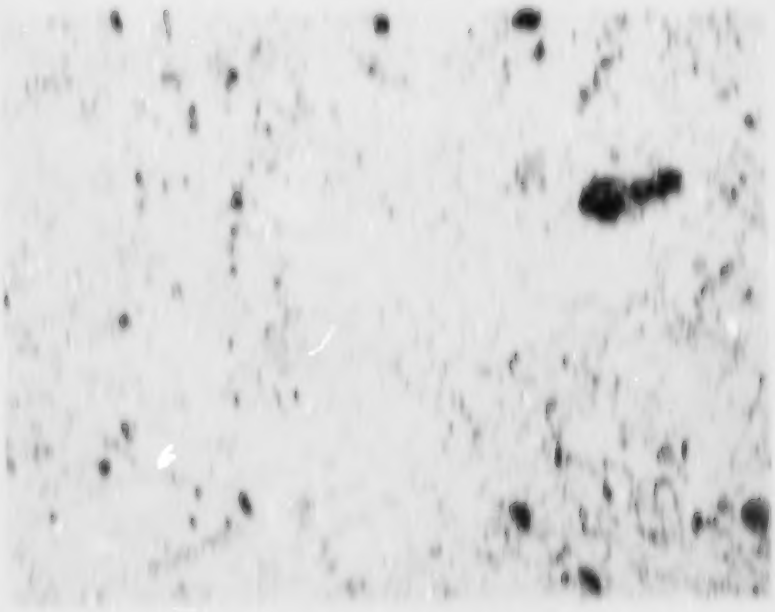

Figure 4. Garrett char. Miscellaneous fine carbon. 100X
Mineral cubes lower left.

Figure 5. Monsanto char. Metallic inclusion upper center. 100X

Fugure 6. Garrett char. 100X
Bright miscellaneous inclusions. Miscellaneous minerals (grey)

TABLE 4. FLUORESCENCE ANALYSIS OF INORGANIC MATERIAL IN CHAR

Element	Wt. % as Oxide
Na	3.11
Mg	14.06
Al	37.74
Si	12.96
Ca	8.51
Ti	0.32
Fe	18.16
Cr and Zr	Present in sample but not in standard
P, S, Cl, K, Mn, Ni, Cu, Zn	Not detected

Figures 12 and 13 show scanning electron photomicrographs at 1000X and 3000X of Garrett char. The inorganic material in Figure 12 was composed principally of K, Ca, and Fe with traces of Al. A crystal of what appears to be calcite appears in Figure 13. Electron fluorescence analysis indicated that Ca was the principal material in this crystal.

Figures 14 and 15 are photomicrographs of sugar char at 100X and 3000X, respectively.

X-Ray Analysis

Char from the Monsanto pyrolysis contained two major crystalline components, α-quartz and a hexagonal phase with lattice constants a = 4.33 Å and c = 17.08 Å. In addition, there were a few very weak unidentified reflections and a pronounced background modulation having a broad peak near d = 3.5 Å, perhaps indicative of the presence of non-graphitic carbon. The structure and parameters of the hexagonal phase were judged to be very similar to those of $CaCO_3$ (calcite), and probably represent a somewhat impure form of this carbonate.

Char produced by the Garrett process also contained α-quartz and impure $CaCO_3$. However, there was significantly less of the carbonate, and it was not as crystalline as in the Monsanto sample. There also appeared to be a larger fraction of non-crystalline material, resulting in a higher background but with a less broadened peak near d = 3.0 Å. It is unlikely that this peak is due to non-graphitic carbon alone, but it probably originates from a mixture of nearly amorphous components.

Because the samples contained particles which had a pronounced magnetic behavior, a crude magnetic separation was effected, and the resulting fractions were examined separately. The magnetic fraction still contained appreciable α-quartz, but none of the carbonate could be detected. Additional weak diffraction peaks were observed which were not present in the patterns of the as-received materials. These peaks

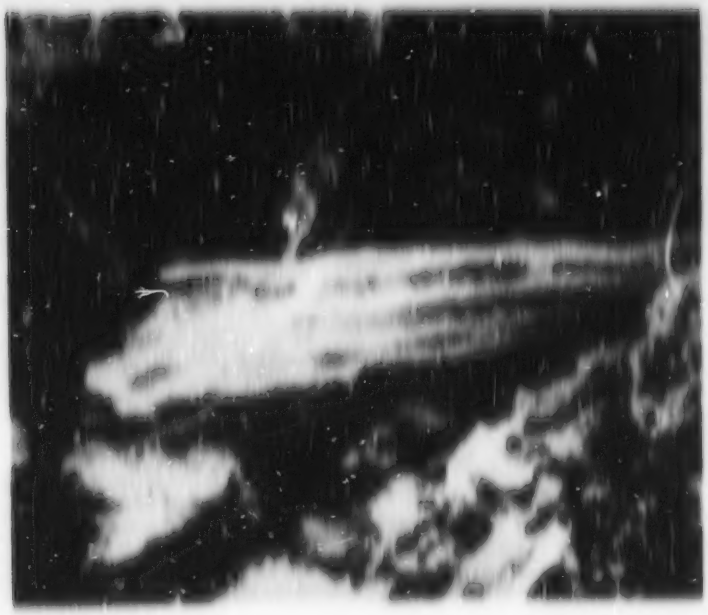

Figure 7. Monsanto char. Probable pyrolyzed wood. 1000X

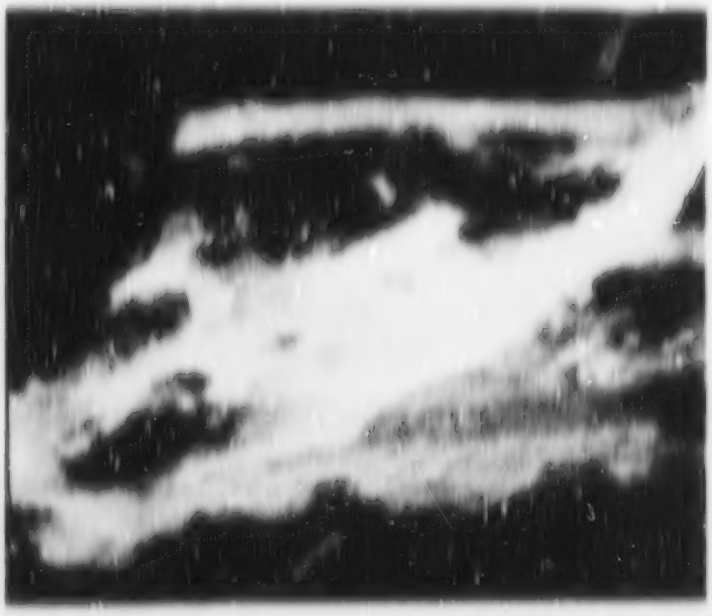

Figure 8. Monsanto char. Probable pyrolyzed wood. 3000X

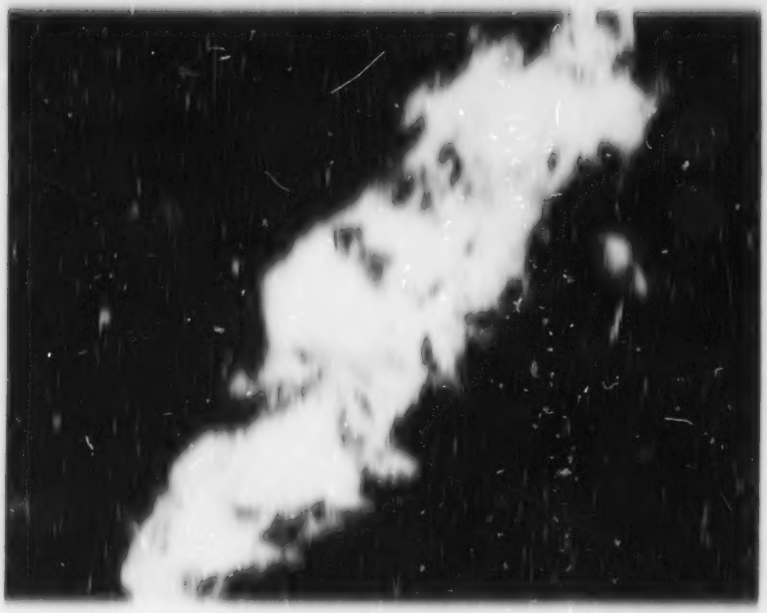

Figure 9. Monsanto char. Principally inorganic matter. 3000X

Figure 10. Monsanto char. Principally inorganic mater. 10,000X

Figure 11. Monsanto char. Principally carbonaceous material. 1000X

Figure 12. Garrett char. Inorganic matter. 1000X

Figure 13. Garrett char. Calcite crystal. 3000X

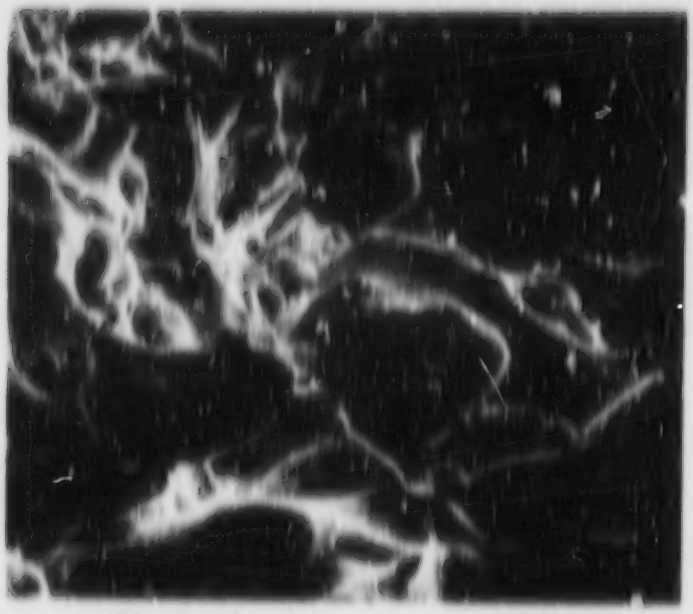

Figure 14. Sugar char. 100X

Figure 15. Sugar char. 3000X

could not be identified as any of the iron-bearing phases listed in the ASTM index, and no further attempts at identification were made.

Density and Surface Area

Results of He density and BET surface area measurements are given in Table 5. For purposes of comparison, the density of amorphous carbon commonly ranges from 1.8 to 2.1 g/cm^3, while that of graphite is about 2.1 - 2.4 g/cm^3. The high density of the Monsanto char may be attributed to its metal and mineral content.

TABLE 5. DENSITY AND SURFACE AREA OF CHARS

Char	Density, g/cm^3	Surface area, m^2/g
Monsanto	2.34	117 ± 9
Garrett	1.69	128 ± 2
Sugar	1.86	636 ± 100

Chemical Analysis

In order to obtain representative samples for chemical analysis, the Monsanto and Garrett chars were coned and quartered following the ASTM Standard Method of Sampling Coke, Designation D-346-36. The Monsanto char, which was high in moisture content (24.4 wt. %), was dried prior to analysis. The Garrett char, which was low in moisture (2.87 Wt. %), was analyzed as sampled.

Samples of the four PERC chars were obtained by splitting the chars as received with a riffle sampler. The samples were then dried to constant weight and milled. Some small flakes of metal that could not be effectively pulverized and homogenized in a mortar were dissolved and reconstituted into the sample.

Results of the analyses for the Monsanto and Garrett chars are given in Table 6, and those for the PERC chars are in Table 7. Elements in the tables are ordered according to the periodic table. With the exception of H, C, N, and S, most of the elements were determined by quantitative spectrochemical analysis, supplemented in a few cases by neutron activation analysis. The sums of the elemental analyses of the Monsanto and Garrett chars were about 63.8 and 78.0 wt %, respectively, and those of the PERC chars were about 72.1, 74.7, 62.2, and 63.1 wt %. The balances are assumed to be largely oxygen bound as metal oxides in the chars. Other than the important differences in the amount of available carbon, the most striking difference between the Monsanto char and the PERC chars is the fact that the Cl content of the latter is an order of magnitude higher.

The only detectable metallic impurity in the sugar charcoal was 0.002 wt. % Si.

TABLE 6. CHEMICAL ANALYSES OF MONSANTO AND GARRETT CHARS
(percent by weight)

Element	Monsanto Char	Garrett Char
H	0.9	2.33
Li	0.002	0.0015
B	0.015	0.004
C	35.4	60.02
N	0.50	0.30
F	0.017	0.006
Na	2.30	0.31
Mg	0.80	0.32
Al	2.80	1.39
Si	11.54	6.04
P	0.5	0.2
S	0.27	0.04
Cl	0.13	0.016
K	1.0	0.6
Ca	4.03	1.58
Ti	0.8	0.6
V	0.006	0.005
Cr	0.05	0.015
Mn	0.2	0.15
Fe	1.96	0.77
Co	0.0015	0.001
Ni	0.61	0.02
Cu	0.1	0.01
Zn	0.2	0.03
Br	0.002	0.0002
Sr	0.05	0.04
Zr	0.02	0.02
Mo	0.003	<0.001
Ag	0.004	0.0002
Cd	0.002	<0.001
Cs	0.0002	0.0001
Ba	0.15	0.05
Hf	0.0037	0.0002
Ta	0.0004	<0.0001
W	0.0008	0.0004
Pb	0.07	0.002
Th	0.0012	0.0002
U	0.0020	0.0065
Ash	54.8	22.7

Elements below the limit of detection:

<0.01	As, Ce, Pr, Nd, Sm, Gd, Tb
<0.003	Nb, Ru, Rh, Pd, Sb, La, Dy, Ho, Tm, Ir, Tl
<0.002	Pt, Au
<0.001	Sc, Ga, Ge, Y, In, Eu, Er, Lu
<0.0006	Hg
<0.0003	Yb
<0.0001	Be

TABLE 7. CHEMICAL ANALYSES OF PERC CHARS
(percent by weight)

Element	#1221-5	#1222-6	#1223-1	#1224-3
H	0.52	0.81	0.32	0.41
Li	0.005	0.0025	0.0016	0.008
B	0.003	0.004	0.01	0.02
C	41.8	51.8	22.6	21.3
N	0.69	1.01	0.19	0.25
F	0.055	0.022	0.049	0.043
Na	2.46	0.84	4.92	3.09
Mg	0.53	0.54	1.01	1.26
Al	3.24	2.85	3.39	2.58
Si	6.2	4.0	20.7	19.0
P	0.05	0.1	0.1	0.05
S	0.1	0.1	0.1	0.1
Cl	2.3	2.6	0.73	0.92
K	2.0	0.6	0.6	2.0
Ca	6.84	6.52	5.13	7.66
Ti	0.4	0.5	0.25	0.5
V	0.002	0.002	0.003	0.006
Cr	0.3	0.05	0.07	0.05
Mn	0.2	0.2	0.2	0.2
Fe	3.3	1.6	1.3	2.7
Co	0.004	0.001	0.001	0.004
Ni	0.04	0.004	0.004	0.01
Cu	0.2	0.06	0.05	0.05
Zn	0.2	0.2	0.3	0.2
Sr	0.05	0.05	0.04	0.07
Zr	0.03	0.006	0.004	0.04
Mo	0.2	0.003	0.001	0.003
Ag	0.0005	0.002	0.0003	0.002
Cd	<0.001	<0.001	<0.001	0.001
Ba	0.1	0.1	0.1	0.2
Pb	0.25	0.15	0.15	0.2
Ash	46.3	34.2	73.6	71.9

Elements below the limit of detection:

<0.1	Ta, W
<0.01	Ga, Nb
<0.005	Sb
<0.001	Ge, In, Bi
<0.0001	Be
<0.00002	Sn

SECTION V

EXPERIMENTAL METHOD

BACKGROUND

The catalyzed or uncatalyzed gasification of various forms of carbon with H_2O or CO_2 is the subject of a very extensive literature. In recent years major concerns have been both to minimize the reactions, if they are between impurities in the helium coolant of high-temperature, gas-cooled reactors and core graphite, or to maximize the reactions, if they are used to gasify coals or chars from various sources. From all this experience, including much fundamental research, certain generalizations relating to the present work are possible.[4,5]

Under otherwise identical conditions, the rate of carbon gasification depends both on the gas composition and on the nature of the carbon surface. When the overall rate of gasification is determined by rates of processes occurring at the carbon surface (which will be the case in this work), rather than by rates of transport of reactant gas to the surface, the relative rates of gas-carbon reactions are roughly in the ratios $1 \times 10^5 : 3 : 1 : 3 \times 10^{-3}$ for $C\text{-}O_2$, $C\text{-}H_2O$, $C\text{-}CO_2$, and $C\text{-}H_2$.

Rate expressions for gasification by H_2O and CO_2 are commonly written in the form[4]

$$\text{Rate}(C + CO_2) = \frac{k_1 P_{CO_2}}{1 + k_2 P_{CO} + k_3 P_{CO_2}} \qquad (6)$$

and

$$\text{Rate}(C + H_2O) = \frac{k_1 P_{H_2O}}{1 + k_2 \frac{P_{H_2O}}{P_{H_2}} + k_3 P_{H_2O}} \qquad (7)$$

These expressions can be derived by postulating reaction mechanisms involving the formation and removal of surface complexes. Their form suggests inhibition of the rates of gasification by the products CO or H_2. Retardation of both reactions by H_2 is generally conceded, but retardation by CO_2 is in some dispute. Study of the above reactions is complicated by the simultaneous occurrence of the water-gas shift reaction (Reaction 3). Rate data for the latter reaction have been fitted to expressions of the form[6,7]

$$\text{Rate}(CO + H_2O) = \frac{k_1 P_{CO}^{1/2} P_{H_2O}}{1 + k_2 P_{H_2O}^{1/2}} \qquad \text{(forward reaction)}, \quad (8)$$

$$\text{Rate}(CO_2 + H_2) = k_1 P_{CO_2} P_{H_2}^{1/2} + k_2 P_{CO_2} P_{H_2}^{1/3} \qquad \text{(reverse reaction)}, \quad (9)$$

Impurities can increase the rates of all these reactions. A significant number of metallic elements or compounds (particularly those of the transition metals and the alkali metal carbonates) catalyze the gasification reactions.[5,6] Also, carbon itself is reported to be a catalyst for the water-gas shift reaction. On the other hand, some of the reactions are subject to poisoning, e.g., by chlorine or boron.

As noted, the purpose of the experimental part of this work is to apply what is known about catalysts of the gasification reactions to char produced by the pyrolysis of solid wastes, and to try to find a catalyst for the commercial application of the process. The direct transfer of results with other sources of char is not immediately obvious, as the ash in the present chars contains both potential catalysts and potential poisons, and the form of the carbon may be different. Because the primary purpose of this research is to identify suitable gasification catalysts, we have not attempted to optimize methane production by the simultaneous addition of methanation catalysts.

EQUIPMENT

Some features of the experimental apparatus were modified during the course of work, and the following description refers to that used for most of the gasification runs.

Runs were made with 1 gram samples mounted in the reactor tube sketched in Figure 16. A photograph of the total system is shown in Figure 17. The reactor tube was fabricated principally of 304 stainless steel and was installed in the system with Swagelok fittings. The char bed was supported on a stainless steel screen, and gas flow was down through the reactor tube. Heating was by a multi-zone furnace capable of temperatures to 800 C. Inlet or reactive gases fed to the reactor tube were metered with calibrated rotameters. Liquid water was pumped with a calibrated Harvard Compact Infusion Pump through 304 stainless steel tubing and vaporized to steam on hot surfaces directly above the reactor tube. Suitable valves prevented back-diffusion and condensation of the steam in other parts of the system. Water in off-gases from the reactor was condensed out with an ice bath, and the flow rate of the

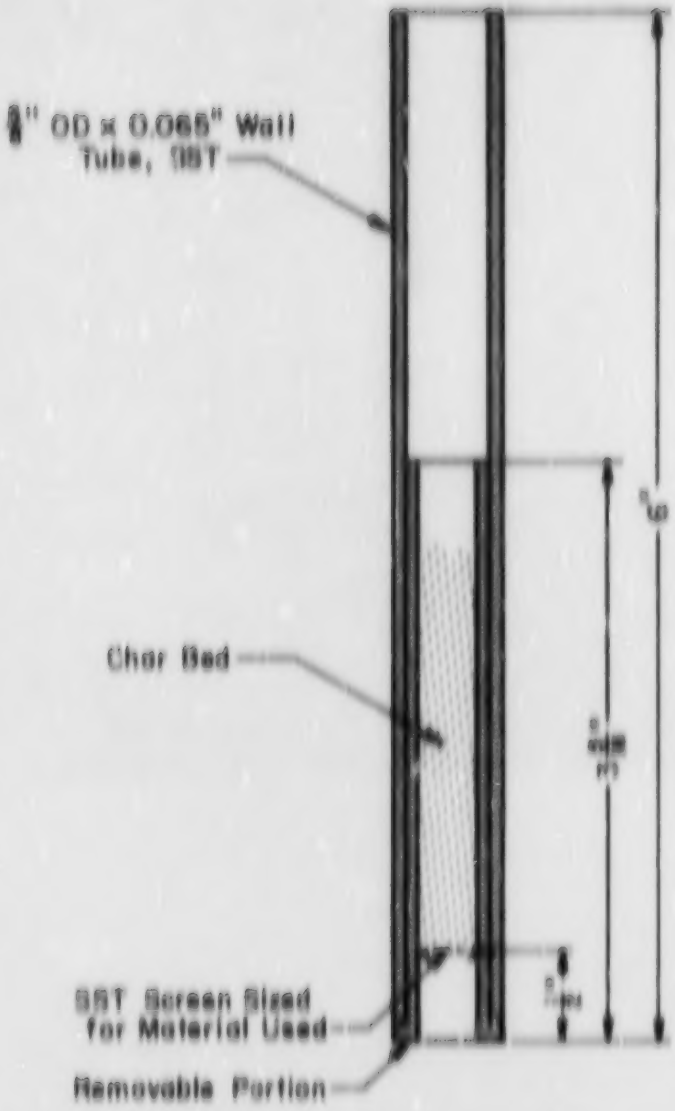

Figure 16. Schematic of gasification reactor tube.

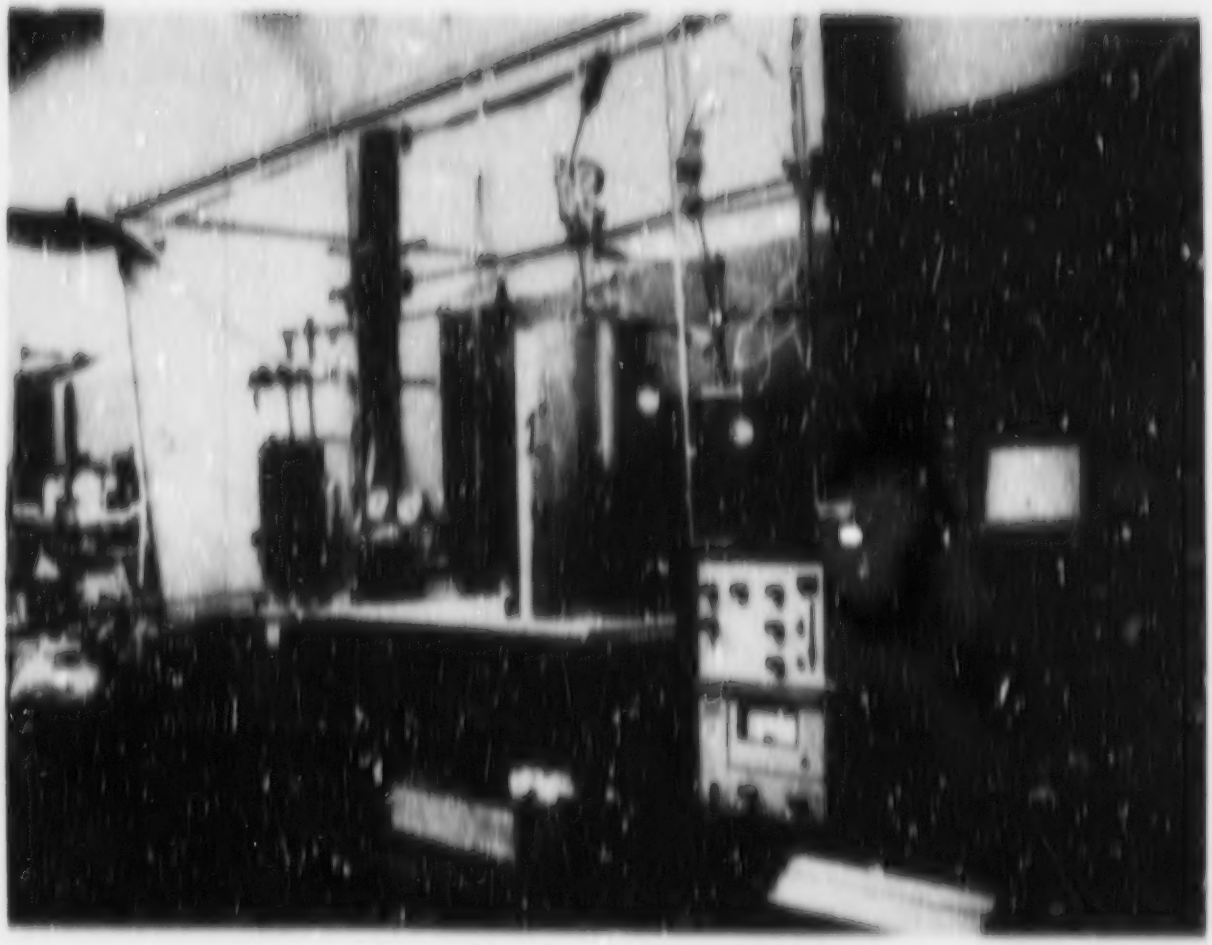

Figure 17. Char reactor equipment.

remaining gases was measured with a following bubble flow meter. Product gases (except water) were periodically analyzed with a Hewlett-Packard Model 5711A gas chromatograph. Initially silica gel was used in the chromatographic columns but Carbosieve B proved to be much more effective in separating the components of the off-gases.

CALIBRATION OF THE CHROMATOGRAPH

The response of the gas chromatograph was calibrated with pure H_2, CO, CO_2, or CH_4 and a number of standardized mixed gases from among those components.

The quantification of chromatographic peaks is usually accomplished by integrating the areas under the peaks. When applied to the calibration of CO, CO_2, or CH_4, the result is a linear plot of peak area versus concentration. However, H_2 is a special problem because the thermal conductivities of H_2 and the column carrier gas, helium, are similar in magnitude. In practice a "normal" positive peak appears for H_2 at low concentrations. At some concentration, ~ 15% in our equipment, the top of the peak flattens. With further increasing H_2 concentrations, a double peak forms, the minimum between the peaks starts back down toward the base line and eventually extends well into the negative direction. Initially we hoped to retain the convenience of a linear plot of concentration versus peak area by defining the area as that of the unfolded peak. This procedure did not give a linear plot. Although still other alternatives are available, we have adopted a non-linear calibration plot of peak height versus concentration, where the peak height is defined as the height of the unfolded peak. The problems of measuring hydrogen by gas chromatography have been discussed by Villalobos and Nuss.[9]

PROCEDURE

The system was brought to temperature (650 C) in the presence of a flowing inert gas, usually helium, before switching to the desired reactant gas mixture. Runs were made at an ambient pressure of about 0.8 atm. Various sequences of gas flows and compositions were used, but a typical run might last 4 hours and consist of the following parts, each lasting one hour and in the indicated order (gas flows measured at 1 atm pressure and room temperature): (1) 10.8 ml/min of CO_2, (2) 10.8 ml/min of He + 0.041? g/min of H_2O (56.6 ml/min of "steam"), (3) 0.041? g/min of H_2O, and (4) 10.8 ml/min of CO_2. The purpose of the fourth part with CO_2 in such a run was to monitor any decrease in the reactivity of the chars over the indicated time interval.

Information available from which to calculate gasification rates includes the weights of char and water consumed as determined from material balances, a comparison of tailpipe gas flows with and without a carrier gas, and the rate of recovery of a gas concentration when

reactant gas composition is changes suddenly.

Because the chars were not taken to exhaustion and each run was started with a fresh batch, the average rates reported are probably higher than would be observed for total gasification of the available carbon.

SECTION VI

EXPERIMENTAL RESULTS

CATALYST MATERIALS

Decision as to which catalysts to test first was based on reported results in the literature for similar systems with due regard for projected catalyst cost and ease of recovery. Because it soon became apparent that the alkali metal carbonates were indeed relatively more effective than other catalysts tested, several attempts were made to improve physical contact between the carbonates and char and hopefully to improve thereby their performance further. The modifications made to the carbonate-char system are included in the following list of catalysts studied:

1) K_2CO_3 and Cs_2CO_3 (Some early work, not reported, was also done with Na_2CO_3.)

2) V_2O_5 (vanadium pentoxide)
The reagent grade chemical was mixed dry with the char.

3) Fe (Metallic iron)
The reduced, reagent grade chemical was mixed dry with the char.

4) $CoMoO_4$ (cobalt molybdate)
This material was obtained as a commercial catalyst, suspended on alumina, from the Houdry Process and Chemical Company. Before use, the as-received pellets were ground and sieved to -35 mesh. The powdered catalyst was then mixed dry with the char.

5) $NiMoO_4$ (nickel molybdate)
The source, received form, and preparation of this commercial catalyst were the same as for the cobalt molybdate.

6) Fly ash
This material had been collected at a commercial, coal-fired power plant and was mixed dry with the char.

7) Li_2CO_3-K_2CO_3
Equal molar mixtures of Li_2CO_3 and K_2CO_3, which melt at about 500 C, were used. Therefore, at the experimental gasification temperature, the catalyst was molten and potentially provided better and more uniform contact with the char. Catalyst was added to the char in two different ways:

a) by slurring the mixture of carbonates in water, adding char to the slurry, and evaporating to dryness,
b) by first making a fused mixture of the carbonates, grinding and sieving the fused salts to -35 mesh, and adding dry to the char.

g) K_2CO_3-DMSO
Dimethyl sulfoxide (DMSO) has remarkable wetting and solubilizing properties. As an alternate method to enhance catalyst coverage of or contact with char, K_2CO_3 was dissolved in an equal volume mixture of DMSO and water; the solution was added to a char sample, and the slurry was dried at 130 C for four hours (K_2CO_3 does not have sufficient solubility in pure DMSO)

For runs with all these materials, 0.1 g of catalyst was mixed with 0.9 g of char. Runs with no catalyst and one run with DMSO alone also used 0.9 g of char.

BLANK RUNS

Two blank runs were made at 650 C with 10.8 ml/min of He (measured at 1 atm and room temperature) and 0.0417 g/min of H_2O. Thus the mol fraction of He was 0.16 and that of steam was 0.84. The first run was made with an empty reactor and the second with 1 g of K_2CO_3 in the reactor. The product gas concentrations quoted below refer to gas chromatographic analysis of streams from which essentially all the H_2O has been trapped out; i.e., they are percents of products referred to He.

EMPTY REACTOR

The major product gas was H_2. At temperature just before addition of water there was 0.2% H_2 in the tailpipe He. The amount increased to 0.8% after 35 min of He-H_2O flow, and then decreased to a steady state 0.4%. The CO_2 started out at 0.6% (presumably due to CO_2 impurity in the He), increased to 0.7%. There were traces of CO and CH_4 (<0.06%).

REACTOR PLUS K_2CO_3

Gas analyses were made for this run during furnace heat up and a He flow of 10.5 ml/min, during 100 min of He + H_2O at temperature, and during furnace cool down under He flow. During furnace heat up and before the addition of H_2O there was a spike of CO_2 in which CO_2 started from 0.6%, increased to 1.8% and decreased to 0.7 ± 0.1%. CO_2 remained at the latter concentration during the remainder of the run. The spike is presumably due to CO_2 adsorbed on the carbonate. The H_2 concentration increased to 0.5% at temperature before the addition of H_2O, it had increased to 1.4% and thereafter decreased slowly during the remainder of the run, becoming undetectable shortly after the H_2O and furnace were turned off. CO and CH_4 were not detected.

CHAR GASIFICATION BY CARBON DIOXIDE

Results for the gasification of chars by CO_2 are summarized in Table 8. The results are arranged in the order of decreasing average percent conversion of CO_2 to CO during the first hour of the runs. The percent conversion is defined as one-half the percent CO in the CO_2. At equilibrium that quantity would be 21.2% under the conditions of the experiments.

There is frequently, but not always, a relatively rapid decrease in the percent conversion during the first 20 min of a run. Also tabulated are the percent conversions observed during the fourth hour for those runs made according to the sequence outlined above as typical. All chars, including sugar char, showed a decrease in the conversion of CO_2 to CO from the first hour to the fourth hour.

TABLE 8. GASIFICATION OF CHARS TO CO BY CO_2

Char	Catalyst	% Conversion to CO 1st hr	% Conversion to CO 4th hr
Synthetic	K_2CO_3	12.3	5.6
Monsanto	pre-fused Li_2CO_3-K_2CO_3	10.5	1.7
Monsanto, acid leached	pre-fused Li_2CO_3-K_2CO_3	10.4	2.3
Garrett	K_2CO_3	6.8	-
Sugar	K_2CO_3-DMSO	7.4	5.1
Monsanto, acid leached	K_2CO_3-	7.1	1.8
Monsanto	Li_2CO_3-K_2CO_3mixture	6.4	1.8
Monsanto	K_2CO_3	6.0	-
Sugar	pre-fused Li_2CO_3-K_2CO_3	5.7	4.6
Monsanto	Fe	5.2	1.0
Monsanto	K_2CO_3-DMSO	4.1	1.0
Monsanto, acid leached	none	3.3	1.4
PERC	K_2CO_3	2.0	-
PERC, acid leached	none	1.8	0.5
Monsanto	V_2O_5	1.8	0.6
Monsanto	CoMoO	1.8	0.5
Monsanto	NiMoO	1.7	0.6
Garrett	none	1.6	-
Sugar	DMSO	1.2	0.4
Sugar	fly ash	1.0	0.2
Monsanto	none	0.8	-
Sugar	none	0.6	0.2
PERC	none	0.6	-

The synthetic char referred to in Table 8 was a sample from a steam pyrolysis experiment on a synthetic solid waste described later in this section. Runs are also listed which were made with acid-leached Monsanto

or PERC chars to determine the effect, if any, of removing potentially catalytic or poisoning inorganic constituents of the chars. The acid leaches were made at 88 C with 60 or 120 ml of 1 N HNO_3 per gram of char followed by three equal volume water washes at the same temperature.

The following conclusions are drawn from the results in Table 8:

The inorganic constituents in the Monsanto, PERC, and Garrett chars have little or no catalytic activity for gasification by CO_2.

Acid-leached chars in the absence of added catalyst have somewhat increased reactivity with CO_2.

The alkali metal carbonates are the best of the catalysts tested. With 10 wt % catalyst, rates of gasification by CO_2 are increased as much as 10 times.

Procedures designed to improve contact of alkali metal carbonates with char do, in general, increase percent conversions.

There is a significant and reproducible variation of results with chars from different sources. The reactivity of subject chars decreased in the order Garrett > Monsanto > PERC.

CHAR GASIFICATION BY STEAM

Results obtained for the rate of gasification of chars by steam are given in Table 9. The data have been arranged in the order of decreasing gasification rates per kg of char, and a column expressing the results per kg of available carbon has been added. Because the various measures of gasification given above in Section V did not always agree, the tabulated rates are probable good only to $\pm$10%.

The PERC char proved somewhat difficult to work with in the steam system. Because the char contained large chunks of metal and other matter, it was necessary to mill the material before all gasification studies. Furthermore, unless the pulverized char was agglomerated with a small amount of water and then dried prior to steam gasification runs, the flow system intermittently plugged.

The major product of steam gasification was a mixture of H_2 and CO_2 at a ratio of about 2:1. With one exception, the amount of CO in the product (measured on a dry basis) was $\leq$ 5% and was usually $\leq$ 2.5%. The exception was the run made with uncatalyzed, acid-leached Monsanto char, in which CO was analyzed to be about 10% of the total (dry) gas. CH_4 production was negligible in all cases.

The small amount of CO produced is consistent with the observed rates of steam gasification and the observed rates of steam gasification and the assumption that, although the gases are not in equilibrium with

TABLE 9. GASIFICATION OF CHARS BY STEAM

Char	Catalyst	Liters of gas/min/ kg of char	Liters of gas/min/ kg of carbon
Sugar	K_2CO_3	7.5	7.5
Sugar	K_2CO_3-DMSO	7.5	7.5
Sugar	pre-fused Li_2CO_3-K_2CO_3	7.5	7.5
Synthetic	K_2CO_3	7.5	13.0
Monsanto	Li_2CO_3-K_2CO_3 mixture	4.8	13.6
Monsanto	pre-fused Li_2CO_3-K_2CO_3	4.7	13.3
Garrett	Cs_2CO_3	4.6	7.6
Monsanto	K_2CO_3	4.5	12.7
Monsanto, acid leached	pre-fused Li_2CO_3-K_2CO_3	4.5	--
PERC	K_2CO_3	4.2	10.0
Monsanto	none	2.9	8.2
Monsanto	Fe	2.6	7.2
Monsanto, acid leached	none	2.4	--
Monsanto, acid leached	K_2CO_3	2.4	--
Monsanto	zeolite	2.3	6.5
Monsanto	K_2CO_3-DMSO	2.3	6.4
Monsanto	$CoMoO_4$	2.3	6.4
PERC	none	1.6	4.5
Monsanto	V_2O_5	1.9	5.3
Sugar	DMSO	1.1	1.1
Sugar	none	0.6	0.6
Sugar	Fly ash	0.4	0.4

solid carbon, the water-gas shift reaction is at or near equilibrium. With the steam flow rate used, the partial pressures of CO_2 and H_2 produced, and an extent of reaction corresponding to gasification rate of, say, 4.5 liters of (dry) gas/kg of char/min, about 4% of the product gas would be CO at equilibrium. This might well be the maximum amount expected, because as the product gases cooled, the amount of CO at equilibrium with other products and steam would be expected to decrease with decreasing temperature until the process became rate limited.

The relatively rapid approach to equilibrium of the water-gas shift reaction was also checked in the reverse direction by passing a 2:1 mixture of H_2 and CO_2 over Monsanto char containing 10 wt % K_2CO_3 at 650 C. The predicted equilibrium constant was satisfied to with 10%.

The following additional observations are made:

The alkali metal carbonates are superior to any of the char catalysts tested.

Acid leaching of chars appears to decrease slightly steam gasification rates. This fact plus other comparisons of data in Table 9 support the conclusion that inorganic material in the chars, particularly in Monsanto char for which more data exist, is itself acting as a catalyst for the reaction with steam. For this reason the increase of gasification rate obtained by adding 10 wt % catalyst is smaller than for gasification with CO_2, and factors of 2 to 3 are observed for Monsanto and PERC chars.

Attempts to improve contact of alkali metal carbonate catalysts with chars and thereby enhance gasification rates by such techniques as lowering the melting point of the catalyst below the gasification temperature were not particularly effective.

When uncatalyzed the relative reactivities of the subject chars with steam again decrease in the order: Garrett, Monsanto, and PERC. When catalyzed, distinctions tend to disappear.

The rates of steam gasification of catalyzed chars obtained here are similar to rates obtained elsewhere for other carbonaceous material under similar conditions; e.g., by Lewis, Gilliland, and Hipkin on K_2CO_3-catalyzed wood charcoal,[10] and by Taylor and Bowman on uncatalyzed coal chars.[11]

SCANNING ELECTRON MICROSCOPY OF PARTIALLY REACTED CHAR

A series of partially reacted sugar chars was examined by scanning electron microscopy. The purpose was to document variations in the form of the deposited catalyst and to correlate this, if possible, with any evidence for a corresponding variation in the nature of the surface reaction. Sugar char was used because the ash content of the other

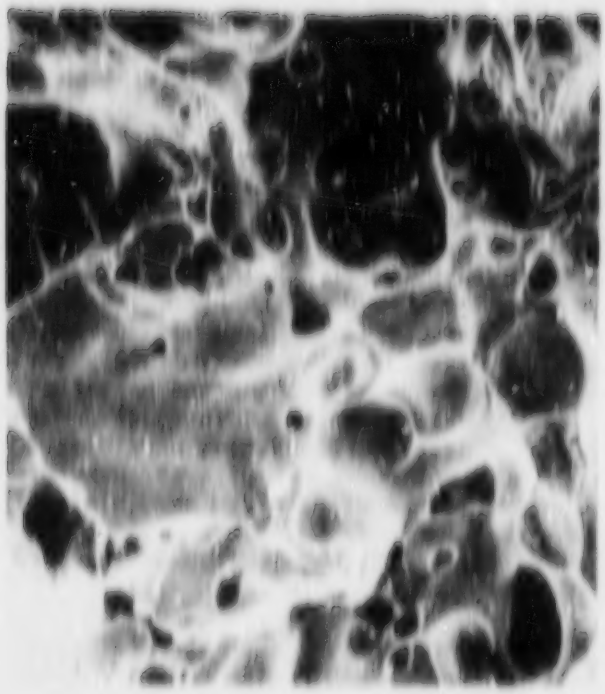

Figure 15. Reacted uncatalysed sugar char. 100X

chars made identification of surface features very difficult.

The unreacted char (Figures 14 and 15) had large, smooth-edged voids and cleavage-type fracture surfaces. The unfractured surfaces were smooth. Figure 16 shows uncatalyzed sugar char that had been reacted at temperatures to 750 C in flowing CO_2. Small, generally lenticular voids are seen, and the cleavage markings on fractured surfaces are not as clearly delineated as in the unreacted sugar char. The large void edges are still generally smooth. In none of the other samples were the lenticular voids as apparent as in this case. Figures 19 and 20 are photomicrographs of sugar char that had been mixed with Cs_2CO_3 catalyst prior to being reacted to temperatures up to 750 C in flowing CO_2. The catalyst was not uniformly distributed, and many char particles had no catalyst on them. The particles containing catalyst appeared to have undergone a considerable amount of reaction adjacent to the catalyst. A few small lenticular voids were present, and cleavage marks were fairly distinct.

The remaining photomicrographs are of partially reacted sugar char exposed to steam. Figure 21 is a photomicrograph of a typical mode of K_2CO_3 deposition by recrystallization when the catalyst was dissolved in water, the solution slurried with sugar char, and the slurry evaporated to dryness. This particular sample had then been partially gasified with a He-H_2O gas mixture. The catalyst was not uniformly distributed. Some particles had little, if any, catalyst, and the particles with catalyst had a nonuniform catalyst distribution. Both rough and smooth-edged voids were present on the catalyst-containing particles. The type of edge, smooth or rough, did not correlate with the presence or absence of catalyst. The particles free of catalyst were generally smooth edged. No lenticular voids were found. In addition to the deposition of the sort shown in Figure 21 the catalyst was also present in some areas as a rounded mass.

Figure 22 is a photomicrograph of sugar char catalyzed with molten Li_2CO_3-K_2CO_3 and then reacted at 650 C with CO_2 and steam. Catalyst was present on all particles, but was not uniformly distributed. Particles low in catalyst had more rough-edged voids than those rich in catalyst. No lenticular voids were found. The catalyst appears to have wet the char, and no deposits of the sort shown in Figure 21 were found.

Catalyst had been deposited on another sugar char sample by evaporating to dryness a slurry of char in a solution of K_2CO_3 in a water-DMSO mixture. The char had then been partially gasified at 650 C with CO_2 and H_2O. Two types of catalyst particles were seen with the scanning electron microscope. Some were very small (~ 1 μ); others were much larger and appeared as columnar growths from the char surface and had striations perpendicular to that surface (Figure 23). The growths were reminiscent of the catalyst particles shown in Figure 21. In general, the surface had a more roughened character than surfaces of the other samples. In addition to some small lenticular voids (1-2 μ) on the

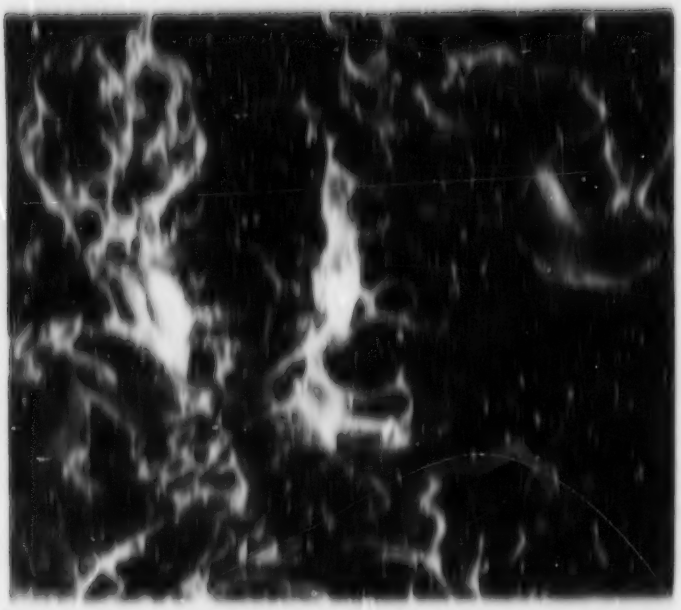

Figure 19. Reacted catalysed sugar char. 100X

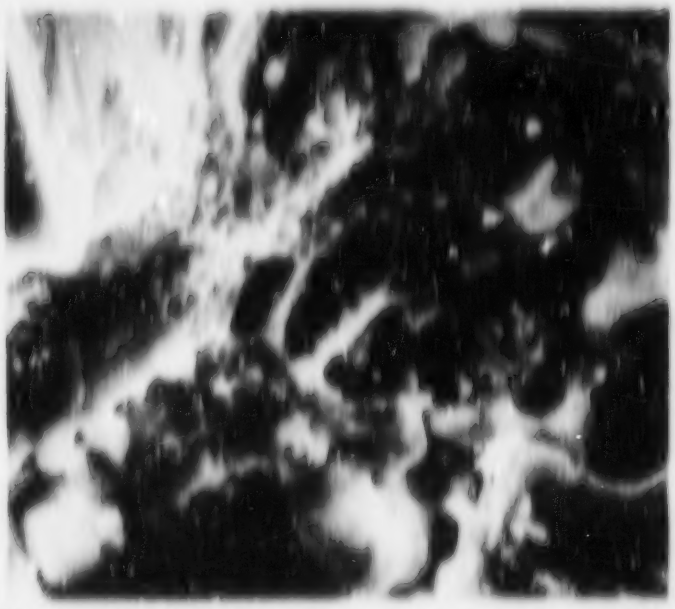

Figure 20. Reacted catalysed sugar char. 3000X

Figure 21. Sugar char. K_2CO_3 catalyst. 1000X

Figure 22. Sugar char. Li_2CO_3 catalyst. 3000X

surface, many other small narrower voids were visible.

Although there are obvious differences in the character of the deposited catalyst in the various samples and some not so obvious divverences in the char surfaces themselves, a correlation with char reactivity does not seem possible at present.

LEACHING OF INORGANIC CONSTITUENTS FROM CHAR

Reference was made above to the preparation of acid-leached Monsanto and PERC chars by extraction with 1 N HNO_3 followed by water washes. We report here the percent of the initial content of several elements in these chars which was so removed, as determined from analysis of combined extraction solutions. Leaching experiments were also made with three equal volume water washes alone, also at 60 C. Results are given in Table 10.

The cases in which greater than 100% of the initial elemental content of the chars was recovered can probably be attributed to the difficulties of sampling heterogeneous chars.

RECOVERY OF CARBONATE CATALYSTS FROM PARTIALLY GASIFIED CHARS

Quarter-gram samples of partially gasified, catalyzed chars from four runs were each leached with three 50-ml portions of distilled water at 60 C as a preliminary test of the feasibility of recovering carbonate catalyst from spent chars. The type of char, catalyst used, and percent catalyst recovered are tabulated in Table 11. The amount of catalyst recovered is based on analyses for lithium and potassium only. The potassium added as catalyst is 10 to 20 times the amount present in the Monsanto char itself when the amount of catalyst added to 10 wt% of the char.

Water is only partially effective for the recovery of catalyst. It is somewhat easier to remove catalyst with water from sugar char than from Monsanto char. The difference may perhaps be explained by the possibility of solid solution formation with oxides or other inorganic compounds in the Monsanto char at gasification temperature.

STEAM PYROLYSIS OF A SIMULATED SOLID WASTE

A single experiment was conducted to explore the response of a solid waste mixture to pyrolysis in a steam atmosphere. For this purpose a cylindrical, electrically heated 1700 watt furnace was used to heat a stainless steel reactor of about one liter capacity which contained 186 g of a simulated solid waste. Water was added to the reactor at the rate of 3.7 ml/min with a peristaltic pump. Exit water and condensable products were collected in a trap, and gaseous products were sampled and later analyzed with a mass spectrometer. The composition of the simulated

Figure 23. Sugar char. K_2CO_3-DMSO catalyst. 3000X

TABLE 10. REMOVAL OF INORGANIC CONSTITUENTS FROM CHAR BY LEACHING

	Percent of Initial Content Removed			
	PERC Char		Monsanto Char	
	Water	1 N HNO_3	Water	1 N HNO_3
Na	30.5	61.0	4.4	26.1
Mg	9.4	94.3	6.2	93.8
Al	0.5	92.6	0.3	71.4
Si	4.0	20.2	2.2	13.0
P	6.0	2500	0.5	90.0
K	37.5	62.5	15.0	40.0
Ca	2.9	87.7	3.7	111.7
Fe	0.003	75.8	0.02	51.0
Cu	0.5	175	0.5	46.0
Zn	0.4	175	0.2	126

TABLE 11. RECOVERY OF CATALYST FROM CHARS

Char	Catalyst	Percent Recovered
Sugar	K_2CO_3	33.2
Sugar	LV_2CO_3-K_2CO_3	96.8 K_2CO_3 62.2 LV_2CO_3
Monsanto	K_2CO_3	25.2
Monsanto	LV_2CO_3	26.1 K_2CO_3 49.0 LV_2CO_3

solid waste is given in Table 12. Water feed was started at a reactor temperature of 150 C, and the temperature was permitted to increase to 750 C over a period of 1 1/2 hours.

TABLE 12. COMPOSITION OF A SYNTHETIC SOLID WASTE

Material	Wt., grams	Material	Wt., grams
paper	53.5	wood	6.2
food	40.3	packaging plastics	5.1
packaging paper	30.2	rubber and leather	4.7
lawn clippings	22.3	plastics	3.3
cloth	22.3		

TOTAL: 188.1 g

The composition of the pyrolysis gas as sampled at various times during the run is given in Table 13. At the lower temperatures, a small amount of tar was trapped, but tar evolution ceased shortly after gas sampling began. At the end of the experiment, 11.3 g of char remained which had the following composition on a dry basis (wt%): C, 57.6; H, 0.73; S, 0.47; N 0.13; ash, 38.6.

It is concluded that solid wastes are amenable to steam reforming and a synthesis gas composed of light hydrocarbons is thereby produced. More research is required to determine optimum temperature and yields.

TABLE 11. ANALYSIS OF VARIANCE FOR SELECTED SPACECRAFT SUBSYSTEMS

Source	df	SS	MS	F	Prob.
Between Groups	4	[illegible]	[illegible]	[illegible]	[illegible]
Within Groups	[illegible]	[illegible]	[illegible]		
Total	[illegible]	[illegible]			

SECTION VII

SYSTEMS STUDY

The objectives of the systems study are to determine the synthetic fuel production potential of the solid wastes produced in this country and to isolate a system that would be suited to the production of hydrogen or methanol from those solid wastes. The system under investigation uses an external heat source to supply the heat required by the endothermic gasification reactions. For purposes of this study, the heat source is anticipated to be a power tower. However, future developments may enable less elaborate solar furnace designs to be used. Also, the candidate solid wastes to be gasified are not limited to chars.

Although the emphasis of the systems study has been on the production of methanol from solid wastes, the merits of producing hydrogen should not be underestimated. The production of ammonia from methane represents between 3 and 4 % of our nation's natural gas demand. The methane is reformed to produce hydrogen, and the hydrogen is used to produce ammonia via the Haber process. Thus, there presently exists a large demand for hydrogen, and producing hydrogen from solid wastes would relieve some of the stress on the nation's natural gas reserves. Economic considerations will ultimately determine whether solid wastes are used to produce hydrogen or methanol.

SYNTHETIC FUEL PRODUCTION POTENTIAL OF SOLID WASTES

At the present time over 90% of our nation's energy demand is met with fossil fuels. During the next sixty-five years we will have exhausted our known natural gas and oil reserves, leaving only coal as a readily available fuel resource.[12] Primary energy sources, such as nuclear, thermonuclear, solar, and geothermal, are expected to make up the difference by the production of electricity and synthetic fuels. Of course, synthetic fuel production will have to depend upon some other source of raw material. But most sources of raw materials are also subject to exhaustion. Perhaps thermochemical hydrogen production will solve this problem by using water as a raw material, but this solution has not yet been proven practical. Therefore, it seems wise to plan for the sustained production of synthetic fuels from our renewable resources to avoid a future fuel crisis.

Solid wastes constitute one of our major renewable resources. Unfortunately, the energy content of solid wastes is small,[13] so that they can only be used to meet a few percent of our nation's energy demand.[14,15]

However, solid wastes can also be used as a raw material for capturing and storing the energy of an external heat source. When used in this manner solid wastes have the potential of meeting over half our entire oil demand in the form of methanol.

Over 50% (by weight) of the wastes discarded in this country consist of hydrocarbons with a primary composition of $C_xH_yO_z$. Sulfur and nitrogen are minor constituents of most solid wastes.[13,16] Under the proper conditions solid wastes react with steam to yield hydrogen and carbon dioxide:

$$C_xH_yO_z + (2x - z)H_2O \rightarrow xCO_2 + (y/2) + (2x - z)H_2 \quad . \qquad (10)$$

Hydrogen has received much attention during recent years as a potential universal fuel.[17-19] Pyrolysis of solid wastes may provide an ideal method for the production of hydrogen. Alternatively, the effluent gases may be used to produce methanol:

$$CO_2 + 3H_2 \rightarrow CH_3OH + H_2O \quad . \qquad (11)$$

Reaction 11 is discussed in Reference 20. Intensive studies of methanol as a gasoline additive are being conducted at several institutions.[21-23]

Table 14 gives the average composition of municipal refuse, and this composition can be used to calculate the hydrogen production potential by using Equation 10. For each kilogram of organic waste converted to hydrogen by equation 10, 1.2 kg of water are required. Thus the high moisture content of organic matter is advantageous for the proposed process. Using the higher heating value of hydrogen, one ton of municipal wastes can produce 7.17×10^4 scf of hydrogen with a heating value of 25×10^6 Btu. This hydrogen can be reacted with the carbon dioxide present in the gas stream to produce 2110 pounds of methanol with a heating value of 20.6×10^6 Btu. The 129 million tons of municipal refuse produced in this country during 1971[14] could have been used to generate 9.25×10^{12} scf of hydrogen with a heating value of 3.3×10^{15} Btu, roughly 15% of the nation's natural gas demand that year. Alternatively, methanol production from the refuse could have yielded 1.36×10^8 tons of methanol with a heating value of 2.67×10^{15} Btu, approximately 12% of our domestic crude oil production during 1971. Tables 15 and 16 present the synthetic fuel production potential of all the solid wastes generated in the U.S.A. during 1971. Clearly, solid wastes represent a significant national resource.

Equation 10 suggests that solid wastes are easily converted to hydrogen and carbon dioxide. Unfortunately, this is not the case. When pyrolyzed in an oxygen-free atmosphere, solid wastes decompose into a variety of gases, tars, oils, liquors, and char.[13] Theoretically, the gaseous and liquid pyrolysis products can be cracked in the presence of

TABLE 14. AVERAGE ANALYSIS OF RAW MUNICIPAL REFUSE

Constituent	Ultimate per cent by weight	
	As received	Dry
Hydrogen	6.2	6.0
Carbon	27.2	47.6
Nitrogen	0.7	1.2
Oxygen	36.8	32.9
Sulfur	0.1	0.3
Ash	7.0	12.0
Btu per pound	4827	8546
Available Btu per ton	9.65×10^6	17.1×10^6

TABLE 15. HYDROGEN PRODUCTION POTENTIAL OF WASTES PRODUCED IN THE USA (1971)

	Wastes generated (10^6 tons)	H_2 (10^{15} Btu)	Readily collectible (10^6 tons)	H_2 (10^{15} Btu)
Manure	700	6.4	26.0	0.83
Urban refuse	120	3.3	71.0	1.80
Logging and wood manufacturing residues	55	1.2	6.0	0.11
Agricultural crops and food wastes	390	6.4	22.6	0.49
Industrial wastes	44	1.2	5.2	0.14
Municipal sewage solids	12	0.4	1.5	0.05
Miscellaneous	60	1.1	5.0	0.11
Totals	880	22.0	136.3	3.53
U.S. natural gas demand (1971)		96		

TABLE 16. METHANOL PRODUCTION POTENTIAL OF WASTES PRODUCED IN THE USA (1971)

	Wastes generated (10^6 tons)	Methanol (10^{15} Btu)	Readily collectible (10^6 tons)	Methanol (10^{15} Btu)
Manure	200	5.2	28.0	0.68
Urban refuse	120	2.7	71.0	1.46
Logging and wood manufacturing residues	55	1.0	5.0	0.09
Agricultural crops and food wastes	390	6.9	22.6	0.40
Industrial wastes	44	1.0	5.2	0.11
Municipal sewage solids	12	0.3	1.5	0.04
Miscellaneous	50	0.9	5.0	0.09
Totals	880	18.0	136.3	2.89
% U.S. oil demand		58		9.3

steam and catalysts at moderately high temperatures to yield hydrogen and carbon dioxide. Experimental verification of this cracking process was recently given by J.L. Cox et al.[15] at the University of Wyoming. An experiment conducted at LASL to study steam pyrolysis of solid wastes is described in Section VI of this report.

As noted in Section III, the char that remains after pyrolysis of the wastes can also be converted to hydrogen and carbon dioxide via the Reactions 1 - 3.

Reactions 1 and 2 are usually observed at temperatures above 800 C; however, catalysts have been used to significantly reduce this temperature.[16,24] Equilibrium constants for the steam gasification reaction (as calculated from thermodynamic data) were given above in Table 1. Our progress in locating suitable catalysts for the practice of Reactions 1 and 2 is described elsewhere in this report. Because approximately 20% of the hydrogen production potential of solid wastes is due to Reactions 1 - 3, the identification of catalysts suited to the practice of these reactions is an important task.

SYSTEMS FOR THE PRODUCTION OF SYNTHETIC FUEL FROM SOLID WASTES

The following paragraphs discuss systems using steam as a reactant for the production of synthetic fuels from solid wastes. The conclusions are equally applicable for carbon dioxide as a reactant. Because the gasification reactions are endothermic, a source of heat is required to drive the reactions. This heat can be supplied either by the sensible heat of the steam or by the use of a heat exchanger to deliver heat directly to the reaction zone. The first method corresponds to adiabatic conditions, and the second to isothermal conditions. The following paragraphs present an analysis of these two methods.

Adiabatic Reactor Design

In the adiabatic case, steam is superheated by a solar furnace (or some other heat source) and pumped through the chemical reactor. Thus, the steam serves as both a heat carrier and a reactant. Characteristics of solar furnaces place an upper bound on the steam outlet temperature of about 700 C. Higher temperatures are achievable, but cause severe materials problems. To provide the heat for Reaction 1 the steam will drop in temperature by an amount ΔT. To ensure that the char is gasified at the required rate the following relationship must be satisfied:

$$\frac{\text{Molar rate of steam flow}}{\text{Molar rate of carbon flow}} \geq (\text{S conversion at } (700 - \Delta T)) \cdot 1. \qquad (12)$$

This assumes that sufficiently good catalysts are located so that the reaction proceeds to equilibrium. Relation 12 puts an effective lower

bound on ΔT. The magnitude of ΔT determines the amount of steam required to provide the heat of reaction.

A computer program was written to do heat and mass balances for combined system. A description and listing of this code are available on request. Representative results are given in Table 17. The stoichiometric steam multiple (SSM) is defined as

$$SSM = \frac{\text{kg of steam/kg of dry organic waste}}{\text{1.2 kg steam/kg of dry organic waste}} \quad (13)$$

where the denominator represents the stoichiometric quantity of steam required to gasify a kilogram of dry organic waste. The initial steam temperature and the amount of char residue remaining after pyrolysis are seen to be critical parameters of the system. If the char percentage can be kept below 10%, or if steam should be available from the solar collector at temperatures exceeding 700 C, the adiabatic system could prove to be practical. Certainly this is the desired conclusion, since an adiabatic reactor would easily combine with present-day solar furnace designs.

Some mention should be made of the uncertainties present in the calculations summarized in Table 17. Only the average specific heat of organic solid wastes was used to calculate the heat required for pyrolysis. Pyrolysis heats of reaction as a function of temperature are not available, and neglect of these heats could change the values of T_f is much greater than room temperature.

TABLE 17. MASS AND HEAT BALANCE CALCULATIONS FOR THE ADIABATIC SYSTEM

% Char	SSM	Temperature, F		
		T_i	T_c	T_f
10	6	650	599	502
10	8	700	597	429
20	10	650	597	527
20	8	700	597	501

SSM = stoichiometric steam multiple
T_i = initial steam temperature
T_c = temperature of gaseous products leaving char gasification zone of reactor
T_f = temperature of gaseous products leaving pyrolysis zone of reactor

Isothermal Reactor Design

A significant fraction of systems study effort was devoted to the design of a practical chemical reactor to be located at the focus of a tower top solar furnace. This reactor design attempts to make use of the unique properties of a solar furnace (which supplies all its heat in the form of radiant light energy) to simplify the intrinsic heat transfer problems and increase efficiency. Although no tower top solar furnaces presently exist in this country, several design studies have been made. ERDA is presently planning for the construction of a 5 MW_{th} test facility and a 30 MW_e production facility. These two facilities are expected to be placed in operation during the next five years. The White Sands Proving Ground in New Mexico has an experimental solar furnace in operation that could be employed for design studies until the 5 MW_{th} test facility becomes operational. Thus ERDA's emphasis on the development of solar process heat technologies points to the timeliness of this research.

Heliostat Economics

Serious design studies of a tower top solar furnace have been made by McDonnell Douglas Astronautics Corporation and the University of Houston.[25] A review of their economic projections is helpful in developing a better understanding of the constraints imposed upon a chemical reactor's design by the solar furnace. A heliostat consists of a 19 m^2 back-silvered flat glass mirror supported by a welded steel frame and a universal mount resting on a pedestal of reinforced concrete. It is estimated that the heliostats comprising the concentrator subsystem of the solar furnace will represent 86% of the total energy collection system cost. Therefore, it is essential that the costs of the heliostat be minimized. Since McDonnell Douglas has already worked on minimizing these costs, we will use their heliostat design in this study.

For a hexagonal heliostat with a span of 4.6 m and an area of 19 m^2, the reflector subassembly cost is estimated to be $246. This estimate includes handling, assembly, and installation costs. The total cost of the heliostat mounting, including guidance, tracking, and control mechanisms, is projected to be $345. The component costs of this subassembly are:

Electronics and sensors	$ 67
Mounting and actuators	104
Pedestal	95
Handling, assembly and installation	79
TOTAL	$345

Other programmatics are expected to add 10% to these costs, bringing the total cost to $650 per heliostat, or $34/$m^2$. More recent studies have suggested somewhat higher costs; however the figures given above are sufficiently accurate for our purpose.

Because the size of the mirror determines the size of the solar image at the focus of the solar furnace, and the size of this image determines the size of the chemical reactor, it is of interest to understand how the heliostat costs vary with mirror size. We make the pessimistic assumption that there would be no decrease in the cost of the mounting subassembly for a smaller heliostat mirror. With this assumption, the cost per square meter for a heliostat with mirror span S_H (in meters) is given by

$$\text{cost/m}^2\ (\$) = 1.1\ \left(12.95 + \frac{18.16}{S_H^2/21.16}\right) \qquad (14)$$

This formula illustrates the simple fact that if the heliostat mirror had an area of 9.5 m^2 rather than 19 m^2, the cost per unit area would increase 60% due to the additional mountings required to achieve the same area coverage (hence the same power output). Thus it makes economic sense to place as large a mirror as possible on each mounting. Factors mitigating against the use of very large mirrors will be discussed in the following paragraphs. Heliostat economics of scale are illustrated in Table 18.

Image Size

The chemical reactor should be located at the focus of the solar furnace to facilitate transfer of heat to the reaction zone. Thus the chemical reactor functions as a heat exchanger in addition to its more obvious role, and its size must be at least as large as the solar image formed at the focus of the solar furnace. The following considerations show how this size limitation places further constraints on the design of the chemical reactor.

TABLE 18. HELIOSTAT ECONOMIES OF SCALE

Heliostat mirror Span, meters	Heliostat cost,[a] $/m²
1.0	437
2.0	120
3.0	61
4.0	41
5.0	31
6.0	26
7.0	23
8.0	21

[a] Cost projections are pessimistic for spans less than 5 m, optimistic for spans greater than 5 m.

Relatively straightforward optical laws determine the diameter of the sun's image D_I to be

$$D_I = (\alpha + \sigma)\frac{2h}{\cos\theta} + S_H \quad , \tag{15}$$

where α is the angle subtended by the solar disc, σ is a measure of the total optical errors associated with the beam reflection by the heliostat, h is the tower height, and θ is the rim angle of the heliostat field from the top of the tower. This formula assumes the flat plate heliostat mirror design studied by the University of Houston and the McDonnell Douglas Corporation. Smaller images are obtained using warped mirror designs currently being developed by Martin Marietta Corporation and the University of Georgia. For these mirrors $D_I \cong S_H$. For present purposes the values of α, σ, and θ are assumed to be 0.009 rad, 0.004 rad, and 63.4°, respectively. These are the same values used by the University of Houston and the McDonnell Douglas Corporation. Substituting these values into Equation 15, we have

$$D_I = 0.0561\,h + S_H \quad . \tag{16}$$

If a land area A_f is needed to collect the desired amount of solar radiation, then the height of the tower required by the solar furnace is given by

$$h \cong \frac{\sqrt{A_f/\pi}}{\tan\theta} = \frac{\sqrt{A_f}}{3.54} \quad . \tag{17}$$

Thus the height of the tower is determined by the power requirement imposed on the solar furnace, and the only remaining "free" parameter in Equation 15 is the span S_H of the heliostat's mirror. But the economics of scale discussed in the paragraphs above limit this span to 4 m or larger; hence the image diameter is effectively determined as

$$D_I \geq 0.0561\,h + 4 \quad , \tag{18}$$

where h is given by Equation 17.

Some reduction in the size of D_I may be possible with more effort to optimize the design of the furnace. The somewhat pessimistic value of σ chosen for this analysis may be reduced as the heliostat guidance system is improved. The rim angle θ cannot be made much larger because of shading effects at the far edge of the mirror field, but some improvements may occur. The analysis presented here is felt to represent a realistic estimate of the solar image diameter as a function of the tower height.

Reactor Design

One potential design for an isothermal reactor uses a quartz "window"

in the chemical reactor to allow the light to pass directly into the reaction zone where it is absorbed by the char and converted to thermal energy. Since char approximates a perfect black body -- it has been used as a source of lampblack -- it is an excellent absorber of solar energy. A fluidized-bed chemical reactor is contemplated due to its excellent heat transfer characteristics. Two reactor geometries are described here; more study will be required to determine the optimum design

The more obvious design, given in Figure 24, uses a cylindrical reactor surrounded by a cylindrical jacket with quartz windows at the bottom of both cylinders. The quartz windows are not intended to be a single solid piece of quartz; rather they are expected to be many quartz plates held together by a metal honeycomb structure. The jacket window is air tight under the modest pressures generated by the compressor. The reactor window however, is perforated to allow the gas reactant (H_2O or CO_2) to fluidize the bed of char and solid wastes. Focused sunlight passing through both windows heats the fluidized bed and enables the pyrolysis and char gasification reactions to proceed.

The most significant drawback of this design is that the diameter D_R of the reactor is larger than D_I and is given by

$$D_R = \frac{D_I}{\cos \theta} = 2.23\, D_I \quad . \tag{19}$$

The surface area S_R is then given by

$$S_R = (D_R/2)^2 = 3.91\, D_I^2 \quad . \tag{20}$$

Because the heat loss due to conduction and radiation is directly proportional to the surface area, this design is potentially less efficient than some others. This design also requires more quartz than other designs, and could be more expensive. In spite of these disadvantages, the design has many attractive features. Conductive heat loss is minimized by the gaseous layer separating the reactor from the jacket. Radiative heat loss is reduced by the absorptivity of quartz, steam, CO_2, CO, etc. in the infrared. The reactive bed is levitated above the quartz window, decreasing the likelihood of chemical reactions between the quartz and the reactants that could cloud the quartz. However, the reactivity of quartz with H_2O, CO_2, CO, H_2, CH_4, etc. at temperatures of 650 C needs further investigation.

A second design, intended to minimize the surface area of the reactor, has also been studied. This design is based on a hemispherical reactor geometry, as shown in Figure 25. Light enters the reactive bed through the walls of the reactor as well as its bottom surface. If we define $R_I = D_I/2$, then

$$\begin{aligned} r &= R_I \sin\theta \\ h &= R_I\,(1 - \cos\theta) \\ v &= \frac{\pi}{2} - \theta \\ H &= R_I \sin\theta\,(2 - \sin\theta) \\ r' &= r + H \sin v \end{aligned} \tag{21}$$

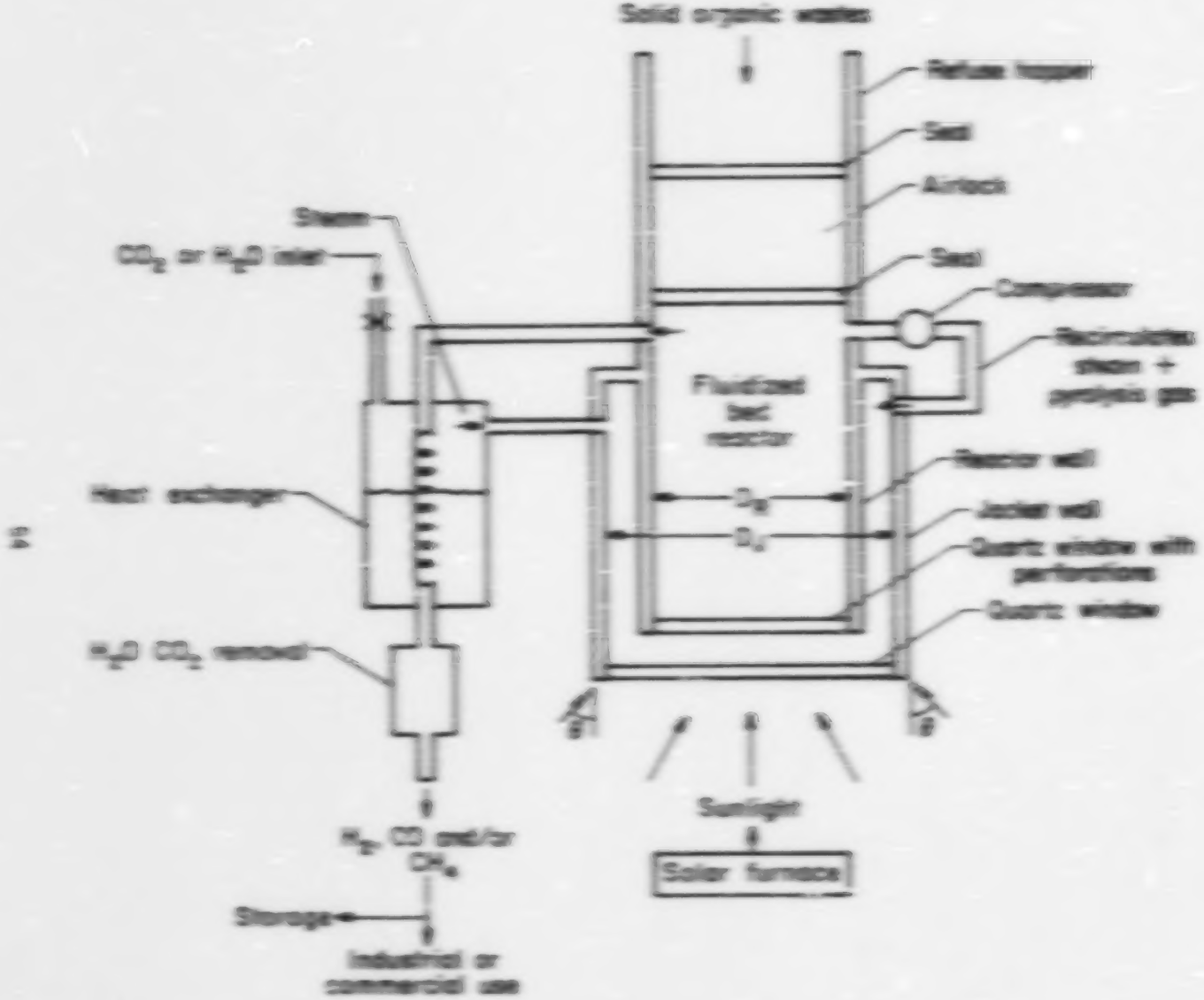

Figure 26. First reactor design.

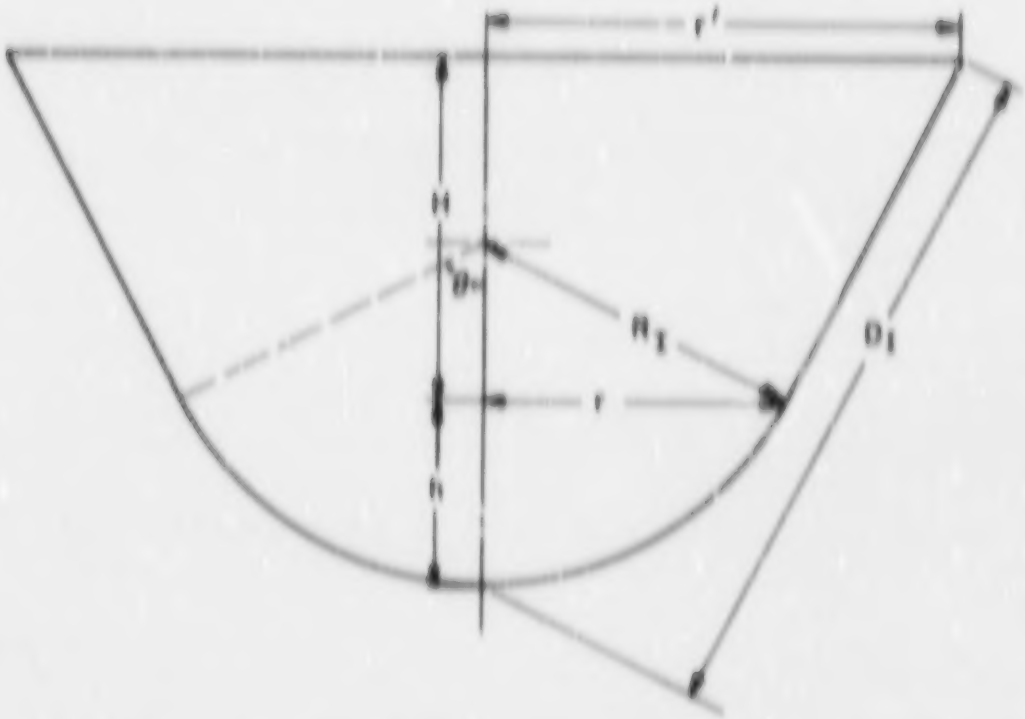

Figure 24. Second reactor geometry

so that the total surface area of the reactor is given by

$$S_H = 2\pi R_1^2(1 - \cos\theta) + \pi(r + r')\sqrt{H^2 + (r - r')^2} \quad . \tag{22}$$

For $\theta = 63.4^\circ$ this becomes

$$S_H = 11.08\,\pi R_1^2 = 2.77\,\pi D_1^2 \quad , \tag{23}$$

representing a 29% decrease in area over the previous case. The volume of this reactor is given by

$$V_H = \frac{2}{3}\pi R_1^3(1 - \cos\theta) + \frac{1}{3}\pi H(r^2 + rr' + r'^2) \quad .$$

This reactor design has most of the advantages attributed to the preceding design and has a smaller surface area. However, it also has several distinct disadvantages. The construction of a hemispherical honeycomb of quartz windows does not appear to be particularly easy. The reactive bed will now be in direct contact with quartz, causing abrasion on the window surface and clouding the quartz. Finally, the reactor has to be full of char at all times, which will be shown to be disadvantageous.

Variations of these two designs are also possible. The inner window of quartz could be replaced by a metal wall with a honeycomb radiant energy absorber attached to it (see Reference 26). In this case the radiant energy would be converted to thermal energy by the absorber and conducted through the metal wall. This appears to be a less desirable method of heat transfer, but may be necessary if the quartz proves to be reactive under working conditions.

The efficiency of this system will be determined primarily by the amount of heat lost from the reactor due to limitations in the reactor's design. Conduction and radiation account for the major losses, with other effects (such as reflection from the quartz windows) contributing to a lesser extent. Estimates of these effects are presented here to provide a better understanding of the system's strengths and limitations.

To estimate conductive heat losses consider two quartz windows of thickness W_q separated by a layer of superheated steam at approximately atmospheric pressure of thickness W_s (see Figure 26). The inner surface of the second quartz window is at a temperature of 15 C. Quartz has a thermal conductivity of 1.4 W/m·K and superheated steam a conductivity of 0.05 W/m·K at 300 C; therefore an estimate of the total conductive heat loss is given by

$$q_c = \frac{638}{2W_q/1.4 + W_s/0.05} \ \text{W/m}^2 \quad . \tag{24}$$

For a reactor with $W_q = 0.01$ m and $W_s = 1.0$ m, the conductive heat loss per square meter is 31.7 W/m^2. Heat loss through the sides and top of the reactor are made negligible by insulation.

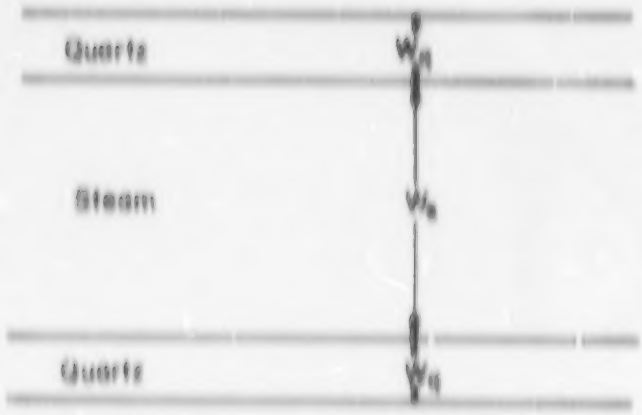

Figure 26. Schematic of window assembly.

If the quartz, steam, and other gases were transparent in the infrared, the heat loss due to radiation would be given by

$$q_r = F\sigma(T + 273)^4 \ W/m^2 \quad , \tag{25}$$

where σ is the Stefan-Boltzmann constant and the angle factor F is given by

$$F = \frac{1}{2}\left(Z - \sqrt{Z^2 - 4X^2Y^2}\right) \quad , \tag{26}$$

where $X = D_r/2W_s$, $Y = 2W_s/D_R$, and $Z = 1 + (1 + X^2)Y^2$. Table 19 illustrates the effect of an increase in the reactor's temperature on radiant heat loss. Clearly there is a significant advantage in practicing the char gasification reaction at lower temperatures. Since the quartz, steam and other reactant gases are not transparent in the infrared and $F \neq 1$, the numbers in Table 19 significantly overestimate the actual heat loss from the reactor.

TABLE 19. EFFECT OF TEMPERATURE ON RADIANT HEAT LOSS BY REACTOR

T, C	Heat loss, W/m^2
550	28.0×10^3
600	32.9×10^3
650	41.2×10^3
700	50.0×10^3
750	62.1×10^3

A fraction of the incident light from the solar furnace will reflect off the quartz window rather than pass through it. Using Fresnel's equations, this loss is estimated to be 4% for light at normal incidence and 10% for light at an incidence angle of 63.4°, for an average loss of 6%. Quartz also becomes less transparent to visible light at higher temperatures, indicating that a non-negligible amount of the radiant energy would be absorbed by the quartz rather than pass through it.

Two solid waste gasification facilities are studied in the following paragraphs: one sized for a tower top solar furnace with a heliostat field radius of 100 m and one with a radius of 200 m, covering land areas of 3.14×10^4 m^2 and 1.26×10^5m^2, respectively. The first yields approximately 7.5 MW_{th} and the second yields 30MW_{th}. A 7.5 MW_{th} facility would be required to gasify the solid wastes of Los Alamos, a community of some 17,000 residents. The larger 30 MW_{th} furnace has been studied by scientists at the University of Houston.

Using Equation 17, the tower height of the 7.5 MW_{th} furnace is 50m.

and that of the 30 MW_{th} furnace is 100 m. The image diameter of the first furnace is determined by Equation 16 to be 7.5 m, and that of the second to be 10.4 m. A chemical reactor sized to the 7.5 MW_{th} facility would require a quartz window surface area of 220 m^2 and the second an area of 423 m^2. Using these figures, heat loss from the two reactors is easily calculated. Comparing the results of Equation 24 with those of Equation 25, it is clear that conduction plays a negligible role in heat loss from the system. This fact illustrates one strength of the jacketed reactor design. Radiant heat loss from the smaller reactor is 8.84×10^6 W at 650 C (assuming no absorption by the gases and quartz) and 16.9×10^6 W for the larger reactor. The smaller reactor loses 0.6×10^6 W due to reflection off the quartz window, and the larger reflector loses 2.4×10^6 W by this mechanism. With these figures, the smaller system has a theoretical efficiency of only 12% and the larger system has a theoretical efficiency of 56%. Fortunately, these figures are not realistic due to the large absorption of infrared radiation by the quartz, steam, and the other gases present in the reactor. Thus the chemical reactor would be considerably more efficient than indicated here. A quantitative estimate of these effects will be made later in this section.

It is also of interest to determine if the kinetics of the carbon-steam reaction are favorable at 650 C. The reaction consumes 0.05 kW-hr/mole (32 kcal/mole) of heat at 650 C. Assuming the 30 MW_{th} solar furnace yields 108 MW-hr of usable heat during a 6-hour day (80% efficiency), 2.06×10^6 moles of C must be consumed each day, or 0.476×10^6 moles/hr. Using a typical reaction rate of 0.09 mole/hr/g_{cat} as determined by experiments described above for synthetic char, the reactor must contain approximately 5000 kg of catalyst and 45,000 kg of char to consume the solar furnace's heat and produce synthesis gas. Using the Garrett char density of 1690 kg/m^3, the required amount of char would have a volume of 26.6 m^3 and would then fill the cylindrical reactor to a depth of 0.063 m. The pressure exerted on the quartz window by the catalyst and char in the reactor would be 1210 nt/m^2 (25.4 lb/ft^2).

It should be emphasized that the preceding calculation is intended only to indicate the feasibility of the design presently being considered. As presented, the calculation must be qualified: 1) the amount of char indicated is an overestimate. Some of the furnace's heat would be used to pyrolyze the solid wastes and provide char for the carbon dioxide - carbon reaction; 2) the reaction rate used was obtained from a fixed-bed reactor. Data from a fluidized-bed reactor are required to make a more realistic calculation.

The preceding calculation also points out a major weakness of the "spherical" reactor design pictured in Figure 25. This reactor needs to be full of char for optimum transfer of heat to the reactive bed. However, a reactor of this design sized to the 30 MW_{th} solar furnace would have a volume of over 900 m^3, much larger than that required by the reaction kinetics. For this reason it seems clear that a design based on a cylindrical reactor geometry is preferable.

Further study of the double quartz window reactor design reveals certain difficulties which could limit its practicality. At high temperatures (such as those encountered on the surface of the inner window) quartz becomes less transparent and more reactive. Without experimental data it is difficult to predict the outcome of these effects on the reactor's operation. Nevertheless, it seemed wise to consider another design patterned on a cavity absorber suggested by W. R. Powell.[27] The following paragraphs describe this new design in some detail.

A brief discussion of the tubular absorber proposed by Powell will be helpful in understanding the reactor described here. As shown in Figure 27 focused sunlight enters the open face of a long quartz tube whose inner surface is coated with a reflective silver film. The light reflects many times down the length of the tube before it is eventually absorbed.

Although the reflectivity ρ of silver is quite high ($\geq$ 0.09), ρ^n is small when the number of reflections n is large enough. The tube loses heat by conduction and infrared radiation; however much of this radiation is absorbed by the quartz tube, so that little escapes out the open face. The reader is referred to Reference 27 for a more detailed description of Powell's invention. The basic thought behind his idea is the use of a reflective surface to achieve absorption of focused sunlight by a great many reflections down the length of the tube.

A chemical reactor having properties similar to the cavity-type absorber may be described as follows. Consider a group of nested annular fluidized-bed reactors as pictured in Figure 28. Each reactor is constructed of a suitable metal with high reflectivity (polished stainless steel for example). Light entering through the open end of the reactor unit is trapped in the cavities separating the annular reactors. As in Powell's design, the light reflects back and forth up the length of the annular opening until it is eventually absorbed on the face of one of the reactor's walls. Thus the annular cavities separating the annular reactors play the same role as the tubular cavity in Powell's design. The reactor unit is jacketed as before and has a single quartz window maintained at a rel relatively low temperature to admit light and retain the reactant gases.

Light enters the reactor with angles (θ measured with reference to the reactor's cylindrical axis) varying between 0° and 63.4°. If the angle θ were too large, much of the light incident on the reactor would reflect out without being converted to heat. On the other hand, if θ is very small the annular reactors have negligible volume. Clearly an optimum angle exists which maximized the annular reactor's volume without sacrificing incident sunlight. A computer program written to determine the optimum angle is described in Appendix A. For a set of annular reactors of radii R_i given by R_i = 0.35 m + i(0.7 m), the optimum angle θ is 1.26° and the optimum height of the annular cone is 1.45 m. The index i runs outward from the center reactor. If the total height of the reactor unit is 10 m, then the ratio of each annular cavity's height to its width is $\approx$ 15.

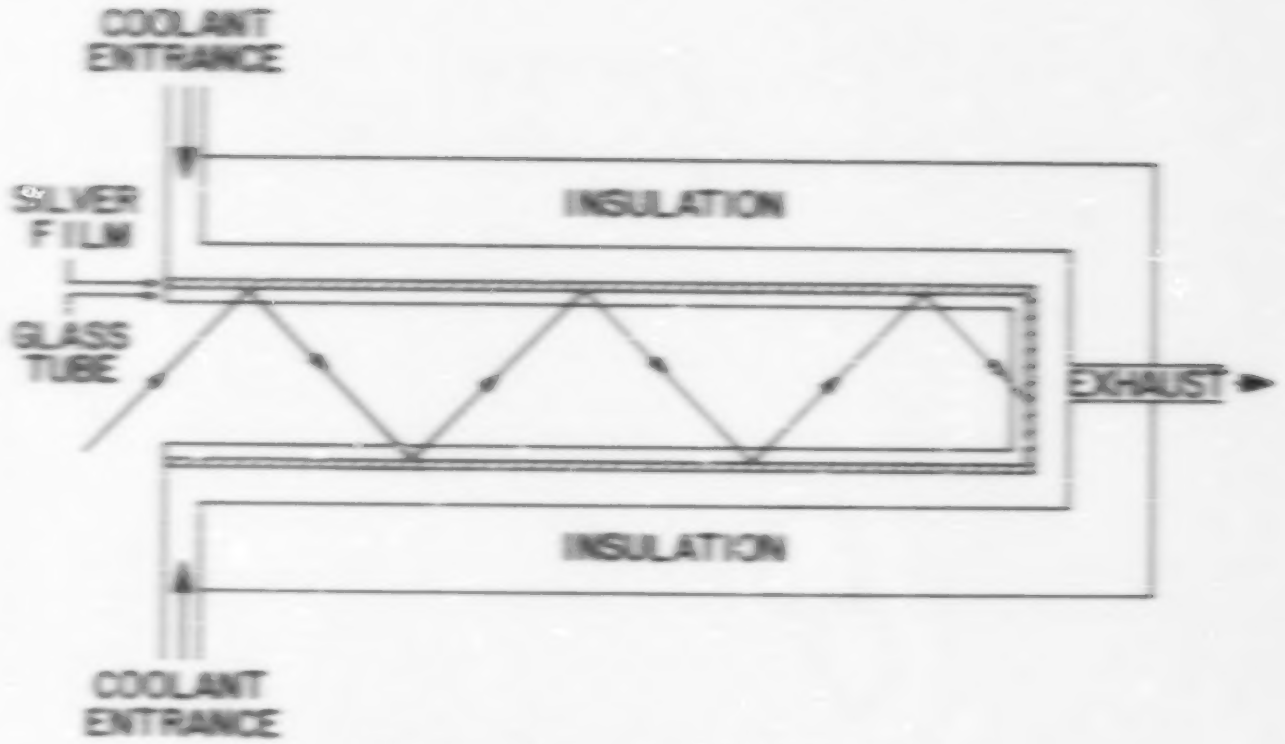

Figure 27. Schematic of a tubular absorber.

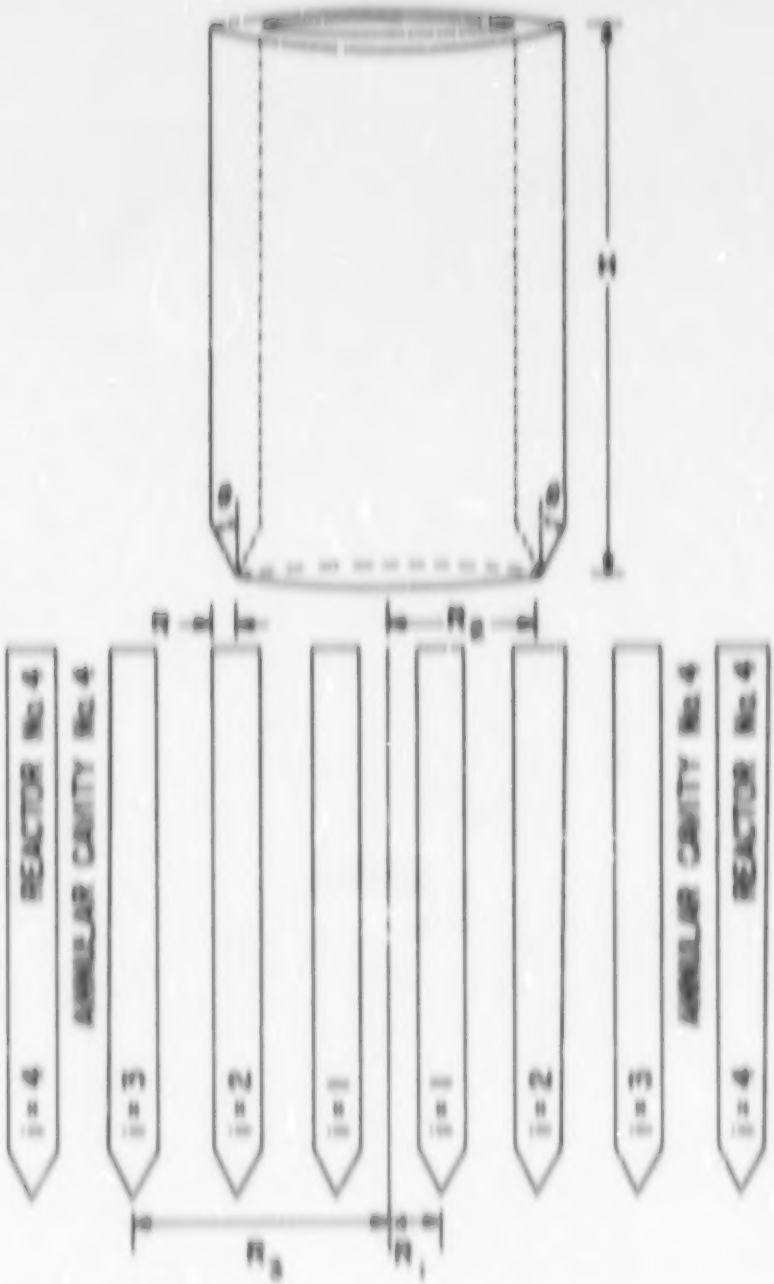

Figure 28. Schematic of a nested annular fluidized-bed reactor.

Powell describes this ratio as adequate to effectively trap radiation incident on the cavity's opening.

The need to retain all the radiation incident on the reactor's lower surface severely restricts the width of each annular reactor and thus limits the total volume of the reactor unit. The size of the solar image at the focus of a 30 MW_{th} tower top solar furnace was shown to be 23.2 m for the McDonnell Douglas design. If the spacing of the annular reactors, R_i, is as given above, then 17 nested reactors are needed to cover the image. The radius R, surface area A, and volume V of each of the annular reactors are given in Table 20, together with sums for the entire unit. The total volume of the unit is seen to be 300.2 m^3, which is more than adequate to contain the 26.6 m^3 of char required to consume the furnace's 30 MW_{th} of heat, taking a catalyzed gasification rate of 0.09 moles/hr/g_{cat} and a carbon/catalyst ratio of 10.

If the reactor's walls are constructed of 1/4" stainless steel, the reactor would weigh 6,400 tons and the char reactant would weigh 60 tons. These numbers are based on the gasification rate obtained for the K_2CO_3 catalyzed $C + H_2O$ reaction and the McDonnell Douglas solar furnace design. Clearly the reactor is much too large for the amount of char required. The size of the reactor is determined by the diameter of the solar image, indicating the desirability of using focusing heliostats (such as those being developed by Martin Marietta) to reduce the image size. Other modifications to present solar furnace designs may also be required to optimize the total system for synthetic fuel production.

It is also of interest to determine the temperature drop across the wall of each annular reactor. The reactor unit has a total area of 12,770 m^2 (137,000 ft^2). If the wall is constructed of 1/4" stainless steel, a temperature drop across the reactor wall of 0.46 C is required to transmit 18 MW_{th} into the reaction zone if it is assumed that the reactor operates at 60% efficiency. Thus the reactor's large surface area permits the transfer of large quantities of energy with a negligible drop in temperature.

To limit radiation losses it is desirable to maintain the open end of the reactor unit at the lowest feasible operating temperature. This is probably best accomplished by introducing the "cold" reactant gas (steam, CO_2, or some mixture thereof) into the bottom of the reactor. Assuming the reactor is used to gasify solid wastes (rather than just the char), the pyrolysis reactions could be practiced in the lower part of the reactor. Elutriation of the fine char particles could provide a mechanism for their movement to the hotter portions of the reactor above the pyrolysis zone.

It would be difficult, if not impossible, to fluidize a bed with a height to width ratio of over 100. Clearly the need is to incorporate several fluidized beds, one above another, in each annular reactor. If a temperature gradient exists along the length of the reactor, as was shown to be desirable in the preceding paragraph, the use of stacked reactors would provide a convenient means for practicing the various pyrolysis and

gasification reactions.

It is to be emphasized that the reactor geometry presented in this section has not been fully optimized. More data on the kinetics of char gasification are required to initiate a truly meaningful design effort. In addition, the intensity distribution of radiation over the solar image is needed to establish the proper location for each annular reactor. Determining the efficiency of this reactor design by estimating its radiant heat loss is an extremely difficult problem. Powell's calculations indicate that his tubular absorber can achieve efficiencies of 90% or better. The purpose of this work was to establish the feasibility of such a reactor and lay the groundwork for a more detailed future study.

It is probably desirable to isolate the chemical reactor from the environment by a glass (or quartz) window. This window lowers thermal losses by conduction, convection, and by retaining a gas mixture of CO_2 and H_2O that is strongly absorptive in the infrared. In addition, the glass window also absorbs strongly in the infrared. These beneficial effects are partially counteracted by radiation losses due to reflection off the two surfaces of the window, and absorption of radiation by the glass. The result of these loss mechanisms is a decrease in the reactor's efficiency, which is traded off against the beneficial effects mentioned earlier. The following paragraphs provide an estimate of the magnitude of these loss mechanisms which can be used to determine the desirability of a windowed reactor versus an open reactor. Neglecting absorption, the transmittance of a single window $\tau_{r,1}$ is given by $\tau_{r,1} = (1 - \rho)/(1 + \rho)$, where ρ is the reflectance of a single glass surface. For small to moderate angles of incidence θ_1, Fresnel's equations can be used to determine the reflectance ρ:

$$\rho = \frac{1}{2}\left[\frac{\sin^2(\theta_2 - \theta_1)}{\sin^2(\theta_2 + \theta_1)} + \frac{\tan^2(\theta_2 - \theta_1)}{\tan^2(\theta_2 + \theta_1)}\right], \tag{27}$$

where $n_1/n_2 = \sin\theta_2/\sin\theta_1$, n_1 is the refractive index of air (n_1=1), and n_2 is the refractive index of glass (n_2 = 1.526). With a mirror field with a rim angle of 63.4°, the average angle of incidence is 45° for approximately equal mirror areas inside and outside the 45° cone. The reflectance ρ for 45° incidence is found to be ρ = 0.054 and the transmittance is then $\tau_{r,1}$ = 0.8975. The transmittance due to absorption losses is given by $\tau_a = e^{-\kappa L}$, where κ is the extinction coefficient for glass and L is the window thickness. For a good quality clear glass κ = 0.04 cm^{-1} and, assuming a window thickness of 5 mm, the transmittance τ_a becomes 0.972. Light absorbed by the glass is turned into heat. With a radiation flux of 30 kW_t over a window area of 423 m^2, the heating rate of the window is 1.89 kW/m^2. The window radiates energy at a rate $\varepsilon\sigma(T^4_{window} - T^4_{surroundings})$, where $\varepsilon \approx 0.94$. Using this expression, a

window temperature of 105 C is required to radiate away the energy received by absorption.

The total transmittance of a single window is given by $\tau = \tau_r \tau_a$. For the conditions assumed here, $\tau = 0.873$. Thus the inclusion of the glass window reduces the reactor's overall efficiency by some 12.7%. To be worthwhile, the window must reduce other thermal losses, and thereby increase the reactor's overall efficiency by at least this amount.

Conduction losses are minimized by surrounding the outer annular reactor with insulation. Assuming the temperature of the outer surface to be 500 C, the insulation to have a conductance of 0.02 Btu/hr·ft^2·°F/ft (glass wool) and a thickness of 0.7 m, the conduction loss is $\sim$ 1.6 kW from the reactor. This trivial amount indicates the importance of minimizing radiation losses.

Estimating radiation losses from a geometry as complex as the proposed design is beyond the scope of this report. However, some insight into the absorption properties of gaseous H_2O and an H_2O,CO_2 mixture can be gained by an analysis of a much simpler problem. Consider two flat, black-body radiators maintained at temperatures T_1 and T_2, where $T_2 > T_1$. The two radiators are separated by a region filled with gaseous H_2O, or a mixture of H_2O and CO_2. If the gaseous H_2O and CO_2 did not absorb radiation, the rate of heat transfer from radiator 2 to radiator 1 would be given by

$$\sigma(T_2^4 - T_1^4) \qquad (28)$$

Assuming radiative equilibrium exists, thereby neglecting conduction and convection mechanisms, we may use the band approximation[20] to estimate the actual rate of heat transfer. The calculation is somewhat complex and is presented in Appendix B. The results are impressive: a one-meter thickness of gaseous H_2O at one atmosphere pressure absorbs 20% of the radiation flowing from radiator 2 to radiator 1 (T_2 = 200 C, T_1 = 100 C). For a mixture of gaseous H_2O and CO_2, over 50% of the radiation is absorbed. Clearly the inclusion of these gases in the reactor's design as a radiative insulator could result in significantly improved performance.

ECONOMICS OF THE PRODUCTION OF SYNTHETIC FUELS FROM SOLID WASTES

In view of the relative lack of information on the economics of solar process heat, it is difficult to provide a realistic estimate of the proposed system. Nevertheless, it is a worthwhile exercise because it reveals what additional knowledge is required to provide such an estimate. The following study presents the economics of a system scaled to the needs of Los Alamos, a community of some 17,000 residents. Refuse collection costs are based on actual experience. If the residents conform to the national average and discard 7 lbs of refuse per day,[14] 50% of which is organic, the community must dispose of 29.75 tons of organic solid wastes

per day.[9] Presently this waste is disposed in a sanitary landfill. We now consider the possibility of using this waste to produce hydrogen for use as a fuel or chemical feedstock.

The average yearly insolation a heliostat is expected to receive in New Mexico is 0.71 kW_{th}/m^2. Collector efficiencies are projected to be approximately 70%;[29] hence the power tower yields 0.50 kW_{th}/m^2 of heliostat mirror area. Gasification of 30 tons of organic wastes is estimated to consume 1.8×10^{11} J of heat over a 6-hour period and to require a furnace with 1.5×10^4 m^2 of heliostats. The furnace and associated facilities would cover about 8 acres of land, which is smaller than the present sanitary landfill. Assuming that the heliostats cost $34.00/$m^2$,[30] the heliostat array is projected to cost $\$525 \times 10^3$. If the tower would cost $\$345 \times 10^3$ and the furnace's total cost would be $\$870 \times 10^3$.

Battelle[32] estimates the cost of a pyrolysis unit and associated support facilities for a community this size to be $\$330 \times 10^3$. Compressors to bring the gas mixture to 275 psia cost $\$400 \times 10^3$, and two shift reactors to remove the CO from the gas stream (if required) cost $\$600 \times 10^3$. Finally, CO_2 is removed by a hot potassium carbonate scrubber costing $\$1.4 \times 10^6$. Some form of low pressure storage will be required to allow the chemical processing facility to operate 24 hours per day (rather than six);however, the cost of such a facility is not available.

Los Alamos probably spends $\$56 \times 10^3$ on labor and $\$30 \times 10^3$ on equipment to collect its refuse per year. It is standard procedure to have two men present at a hydrogen processing facility at all times, increasing the labor cost to $\$156 \times 10^3$. Maintenance at 5% per year would cost $\$180 \times 10^3$, and the compressor's electrical consumption is estimated to cost an addition $\$53 \times 10^3$.

To cover the project's capital costs, we assume the community would issue $\$3.6 \times 10^6$ of municipal bonds at 7% interest with an amortization period of twenty years. Principal plus interest payments on the bonds would cost $\$336 \times 10^3$. Communities are presently[33] generating their own electrical power from "municipalized" utilities, so the idea is not un--realistic. With revenues of $8.00 per ton for solid waste collection paid by the residents, the community would break even if it sold the 236×10^9 Btu of hydrogen produced yearly for $2.90 per million Btu. These results are summarized in Table 21. If the solar furnace should cost three times the amount indicated in Table 21, hydrogen would have to be sold at $3.80 per million Btu to break even.

[9]Although 7 lbs of refuse per person per day may appear high when compared with other studies, we are assuming that 3.5 lbs of organic wastes are available per day from the residents. Because sewage sludge could be used to supplement the refuse collected, this is a reasonable assumption.

TABLE 20. DIMENSIONS OF ANNULAR REACTORS

Index No. of Annular Reactor	Radius, m	Area, m^2	Volume, m^3
1	0.38	44.8	1.04
2	1.05	132.0	3.13
3	1.78	220.9	5.21
4	2.48	309.3	7.30
5	3.15	397.6	9.38
6	3.85	486.0	11.47
7	4.55	574.3	13.55
8	5.25	662.7	15.64
9	5.95	751.1	17.72
10	6.65	839.4	19.81
11	7.35	927.8	21.89
12	8.05	1016.2	23.97
13	8.75	1104.5	26.06
14	9.45	1192.9	28.14
15	10.15	1281.2	30.23
16	10.85	1371.0	32.3
17	11.55	1459.0	34.4
	TOTAL	12,770	300.2

TABLE 21. ECONOMIC ANALYSIS OF A MUNICIPAL SYNTHETIC FUEL PLANT

Capital Costs (10^6)		
Heliostats	0.53	
Tower	0.34	
Pyrolysis Reactor and Associated Plant	0.33	
Compressors	0.40	
Shift Reactors	0.60	
Scrubber	1.40	
	3.60	TOTAL
Operating Costs (10^6)		
Principal and 7% Interest	0.334	
Labor	0.156	
Equipment and Maintenance	0.210	
Compressor (electricity)	0.063	
	0.763	TOTAL
Revenues (10^6)		
Refuse Collection	0.066	
Hydrogen (269 x 10^9 Btu with 80% availability at $2.90/$10^6$ Btu)	0.687	
	0.753	TOTAL

To some extent the foregoing represents a "worst case analysis" due to the dis-economies of scale present for such a small community. Larger communities could manufacture hydrogen less expensively because equipment and operating costs would be proportionally less. Nevertheless, some pressing technological questions remain. Power towers generate steam at high pressures, but little is known about solid waste pyrolysis in a pressurized steam atmosphere. Production of hydrogen under pressure could greatly reduce compressor costs, but would increase the cost of the pyrolysis reactor. More accurate estimates of the heat required for pyrolysis are needed, and the costs and recoverability of catalysts for char gasification need to be investigated. Some features of present power tower designs will probably have to be altered to suit the needs of chemical processing technology. Although some pessimistic assumptions were made during this study, solar process heat may prove to be much more expensive than present projections. Nevertheless, this analysis suggests that the application of solar process heat to fuel production may be a technology whose time has come.

SECTION VII

REFERENCES

1. Huang, C. J., and Dalton, C., "Energy Recovery from Solid Wastes," Summary Report, Volume 1, and Technical Report, Volume 2, NASA CR-2526, April 1975.

2. JANAF Thermochemical Tables, M. W. Chase, Project Director, Dow Chemical Company, Midland, MI, looseleaf and supplements.

3. Marvin, G., Inorganic Syntheses, Volume II, W. C. Fernelius, Editor, McGraw-Hill Book Company, Inc., New York (1946), page 74.

4. Walker, P. L., Rusinko, F., and Austin, L. G., "Gas Reactions of Carbon," Advances in Catalysis, Volume XI, D. D. Eley, P. W. Selwood, and P. W. Weisz, Editors, Academic Press, New York (1959), page 133.

5. Walker, P. L., Shelef, M., and Anderson, R. A., "Catalysis of Carbon Gasification," Chemistry and Physics of Carbon, Volume 4, P. L. Walker, Editor, Marcel Dekker, New York (1968), page 287.

6. Graven, W. M. and Long, F. J., "Kinetics and Mechanisms of the Two Opposing Reactions of the Equilibrium CO + H_2O = CO_2 + H_2," J. Amer. Chem. Soc. 76, 2602, 6421 (1954).

7. Tingey, G. L., "Kinetics of the Water-Gas Equilibrium Reaction. I. The Reaction of Carbon Dioxide with Hydrogen," J. Phys. Chem. 70, 1406 (1966).

8. Krueger, C., "The Gasification of Carbon by Air, Carbon Dioxide and Steam and the Effect of Inorganic Catalysts," Z. Angew. Chem. 52, 729 (1939).

9. Villalobos, R. and Nuss, G. R., "Measurement of Hydrogen in Process Streams by Gas Chromatography," ISA Trans. 4, 291 (1965).

10. Lewis, W. K., Gilliland, E. R., and Hipkin, H., "Carbon-Steam Reaction at Low Temperatures," Ind. Eng. Chem. 46, 1697 (1953).

11. Taylor, R. W. and Bowman, D. W., "Rate of Reaction of Steam and Carbon Dioxide with Chars Produced from Subbituminous Coals," Lawrence Livermore Laboratory Report UCRL-52002, January 1976.

12. Rubin, E. S., "Research and Development Needs for Enhancing U. S. Coal Untilization," Proc. Ninth Intersociety Energy Conversion Engineering Conference, San Francisco, Calif.; Inst. Electrical and Electronic Engineers, New York (1974), page 997.

13. Saner, W. S., Ortuglio, C., Walters, J. G., and Wolfson, D. E., Conversion of Municipal Wastes and Industrial Refuse into Useful Materials by Pyrolysis," U. S. Bureau of Mines Report of Investigations 7428 (1970).

14. Anderson, L. L., "Energy Potential from Organic Wastes: A Review of the Quantities and Sources," U. S. Bureau of Mines Information Circular 8549 (1972).

15. Maugh, T. H., "Fuel from Wastes: A Minor Energy Source," Science 178, 699 (1972).

16. Cox, J. L., Hoffman, E. J., Hoffman, R. W., Wilson, W. G., Roberts, J. A., and Stinson, D. L., "Gasification of Organic Waste," Amer. Chem. Soc., Div. Fuel Chem., Prepr. 18(1), 1 (1973).

17. DeBeni, G. and Marchetti, C., "Hydrogen, Key to the Energy Market," Euro-Spectra 2, 46 (1970).

18. Gregory, D. P., "The Hydrugen Economy," Sci. Amer. 228(1), 13 (1973).

19. Gregory, D. P., Ng, D. Y. C., and Long, G. M., "The Hydrogen Economy," The Electrochemistry of Cleaner Environments, J. O'M. Bockris, Editor, Plenum Press, New York (1972), page 226.

20. Woodward, H. F., "Methanol," Encyclopedia of Chemical Technology 13, 379 (1967)

21. Reed, T. B. and Lerner, R. M., "Methanol: A Versatile Fuel for Immediate Use," Science 182, 1299 (1973).

22. Wigg, E. E., "Methanol as a Gasoline Extender: A Critique," Science 186, 785 (1974).

23. Reed, T. B., Lerner, R. M., Hinkley, E., and Fahey, R., "Improved Performance of Internal Combustion Engines Using 5 - 30% Methanol in Gasoline," Proc. Ninth Intersociety Energy Conversion Engineering Conference, San Francisco, California Inst. Electrical and Electronic Engineers, New York (1974), page 952.

24. Haynes, W. P., Gastor, S. J., and Forney, A. J., "Catalysis of Coal Gasification at Elevated Pressure," Coal Gasification, L. G. Massey, Editor, Adv. in Chem. Series 131, Amer. Chem. Soc., Washington, D. C. (1974), page 179.

25. Vant-Hull, L. L., "Solar Thermal Power Systems Based on Optical Transmission," Semiannual Progress Report, 15 June - 31 Dec. 1973, Office of Tech. Services Report PB-237006/4 (1974).

26. Francia, G., "Pilot Plants of Solar Steam Generating Stations," Solar Energy 12, 51 (1968).

27. Powell, W. R., "Absorber for Solar Power," Appl. Optics 13, 2430 (1974).

28. Sparrow, E. M. and Cess, R. D., Radiation Heat Transfer, Brooks-Cole Publ. Co., Belmont, Calif. (1966).

29. Blake, F. A., "Solar Augmentation of Hydroelectric Power Systems," Energy Sources 1, 361 (1973-74).

30. Easton, C. R., Hallet, R. W., Gronich, S., and Gervais, R. L., "Evaluation of Central Solar Tower Power Plant," Proc. Ninth Intersociety Energy Conversion Conference, San Francisco, Calif., Inst. Electrical and Electronic Engineers, New York (1974), page 271.

31. Woodcock, G. R. and Gregory, D. L., "Economics Analyses of Solar Energy Utilization," Proc. Ninth Intersociety Energy Conversion Conference, San Francisco, Calif., Inst. Electrical and Electronic Engineers, New York (1974), page 306.

32. Hammond, V. L., Mudge, L. K., Allen, C. H., and Schiefelbein, G. F., "Energy from Solid Wastes by Pyrolysis-Incineration," Battelle Pacific Northwest Laboratories Report BNWL-SA-4471 (1972).

33. Anon., "Is Municipal Power the Answer?," Business Week, Jan. 20, 1975, page 50.

APPENDIX A

OPTIMIZATION OF THE REACTOR'S VOLUME

Light enters the cylindrical annular reactor with angles varying between 0 and 63.4 , as shown in Figure 29. If the angle is small enough, the light reflects off the wall of the reactor as shown in the figure and continues to progress deeper into the annular cavity separating two of the reactors. However, when θ is too large, the light reflects out of the cavity rather than deeper into it. The volume of the reactor is also determined by θ . A larger angle θ gives a larger reactor volume. The purpose of this appendix is to describe an algorithm for maximizing the reactor's volume while retaining all the radiation incident on it from the solar furnace.

To solve this problem we examine the "worst case", as shown in Figure 29. Light strikes the "point" of the left annulus with angle $\theta = 63.4^{\circ}$. It is reflected with angle

$$\phi_1^L = 180^{\circ} - 2\theta - \phi_1^L \quad , \tag{29}$$

where $\phi_1^L = \theta = 63.4^{\circ}$ is the angle of incidence on the left annulus for the first reflection. This beam of light is incident on the right surface of the annular cone with angle $\phi_1^R = 180^{\circ} - 2\theta - \phi_1^L$. It reflects off the right surface with angle

$$\phi_1^R = 180^{\circ} - 2\theta - \phi_1^R \tag{30}$$

and is incident on the left surface with angle $\phi_2^L = 180^{\circ} - \phi_1^R$. We now have an iterative scheme for determining the angles ϕ_n^L, ϕ_n^R, ϕ_{n+1}^L, ϕ_n^R as a function of the $2n - 1$ and $2n$ reflection number. Our desire is to keep either ϕ_n^R or ϕ_n^L greater than 90°, which constrains the number of reflections n allowed.

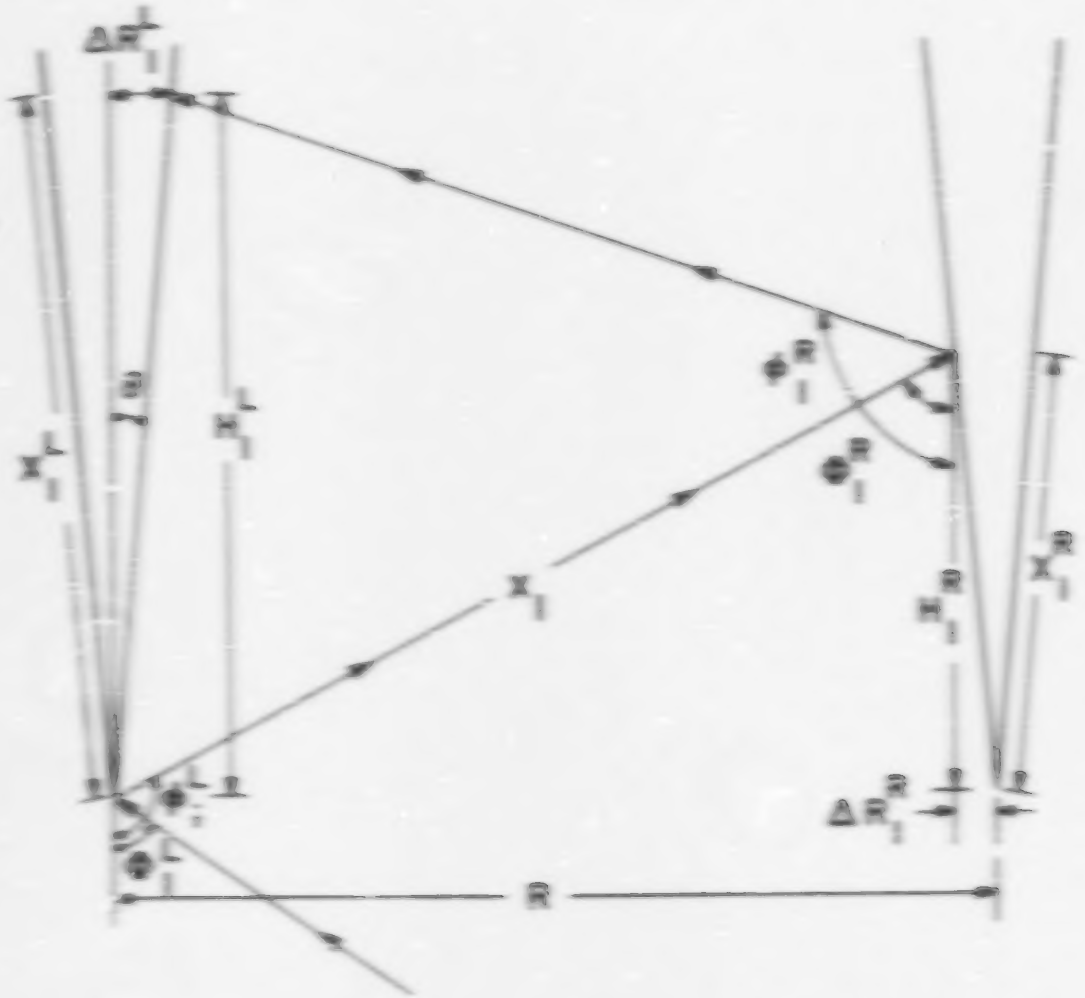

Figure 25. Light reflection between two mirror surfaces.

the distance x_1^R is given by

$$x_1^R = \frac{R \sin(\phi_1 - 90^\circ) \sin(180^\circ - \phi_1)}{\sin(\phi_1 - \theta)} \quad , \tag{31}$$

and the height H_1^R by

$$H_1^R = x_1^R \cos\theta \quad , \tag{32}$$

with distance

$$\Delta R_1^R = x_1^R \sin\theta \quad . \tag{33}$$

The distance x_1 is now seen to be

$$x_1 = H_1^R / \sin(\phi_1 - 90^\circ) \quad . \tag{34}$$

and the values of x_1^1, H_1^1, and ΔR_1^1 are given by

$$x_1^1 = \frac{x_1 \sin(\phi_1^R + \phi_1 - 180^\circ)}{\sin(180^\circ - \phi_1^R + \theta)} \tag{35}$$

$$H_1^1 = x_1^1 \cos\theta$$

$$\Delta R_1^1 = x_1^1 \sin\theta \quad .$$

If the total height of the reactor is 10 m and R = 0.7 m, we now have an iterative scheme for determining the volume of the reactor V as a function of the number of reflections n and the angle of incidence θ. Values given in the body of this report were obtained using a computer program designed to optimize V for a given value of θ.

APPENDIX B

RADIANT HEAT TRANSFER IN GASEOUS H_2O AND CO_2 + H_2O MIXTURES

A description and derivation of the band model for the exponential kernel solution to the radiative equilibrium problem is beyond the scope of this report. Such a derivation is given by Sparrow and Cess in their book *Radiation Heat Transfer* on pp. 239-247.[28] Using their formulas, gaseous water with the band structure

λ	$\Delta\lambda$
1.38μ	0.18μ
1.37	0.3
2.7	0.29
6.3	2.0
20.	8.0

and a thickness of 1 m absorbs 26.6% of the infrared radiation leaving a black body radiator at 650 C. An equi-molar mixture of CO_2 and gaseous water with a total pressure of 2 atm and a band structure

λ	$\Delta\lambda$
2.7μ	0.6μ
4.3	1.2
15.	10.9

with a thickness of 1 m absorbs 59.3% of the radiation leaving a black body at 650 C. These calculations indicate the effectiveness of CO_2 and gaseous H_2O as a radiation insulator.